



12-1985

The Design and Construction of Microprocessor-Computer Controlled Rapid Scanning Fiberoptic Spectrophotometer

Kathleen Marie Tobin

Follow this and additional works at: https://scholarworks.wmich.edu/masters_theses



Part of the Chemistry Commons, and the Optics Commons

Recommended Citation

Tobin, Kathleen Marie, "The Design and Construction of Microprocessor-Computer Controlled Rapid Scanning Fiberoptic Spectrophotometer" (1985). *Master's Theses*. 1472.

https://scholarworks.wmich.edu/masters_theses/1472

This Masters Thesis-Open Access is brought to you for free and open access by the Graduate College at ScholarWorks at WMU. It has been accepted for inclusion in Master's Theses by an authorized administrator of ScholarWorks at WMU. For more information, please contact wmu-scholarworks@wmich.edu.



**THE DESIGN AND CONSTRUCTION OF MICROPROCESSOR-COMPUTER
CONTROLLED RAPID SCANNING FIBER OPTIC SPECTROPHOTOMETER**

by

Kathleen Marie Tobin

**A Thesis
Submitted to the
Faculty of The Graduate College
in partial fulfillment of the
requirements for the
Degree of Master of Arts
Department of Chemistry**

**Western Michigan University
Kalamazoo, Michigan
December 1985**

THE DESIGN AND CONSTRUCTION OF A MICROPROCESSOR-COMPUTER
CONTROLLED RAPID SCANNING FIBER OPTIC SPECTROPHOTOMETER

Kathleen Marie Tobin M.A.

Western Michigan University, 1985

Conventional spectrophotometers require the transfer of a sample to a cuvette for obtaining spectra. The measurement of absorbance in situ can be accomplished using a fiber optic probe which can be placed directly into the sample. The fiber optic probe also minimizes environmental factors such as thermal or vibrational which may affect the absorbing species. A rapid scanning speed allows for essentially simultaneous wavelength monitoring.

The effect of coupling a rapid scanning spectrophotometer with a fiber optic probe provides for an extremely versatile system. When used in conjunction with a microprocessor or computer, this approach offers advantages such as data manipulation, time averaging of signals, low signal-to-noise ratios while retaining high precision, dynamic range, and resolution.

ACKNOWLEDGEMENTS

A special acknowledgement to my research advisor, Dr. James Howell, whose knowledge, support, guidance, and patience has added much to my ability to carry out research. The Chemistry Department at Western Michigan University has been very generous with its extremely limited budget for the purchase of the necessary components and their support in the form of teaching assistantships. Finally, I wish to thank my parents, Mr. and Mrs. John Tobin, for their patience and continuous moral support.

Kathleen Marie Tobin

INFORMATION TO USERS

This reproduction was made from a copy of a document sent to us for microfilming. While the most advanced technology has been used to photograph and reproduce this document, the quality of the reproduction is heavily dependent upon the quality of the material submitted.

The following explanation of techniques is provided to help clarify markings or notations which may appear on this reproduction.

1. The sign or "target" for pages apparently lacking from the document photographed is "Missing Page(s)". If it was possible to obtain the missing page(s) or section, they are spliced into the film along with adjacent pages. This may have necessitated cutting through an image and duplicating adjacent pages to assure complete continuity.
2. When an image on the film is obliterated with a round black mark, it is an indication of either blurred copy because of movement during exposure, duplicate copy, or copyrighted materials that should not have been filmed. For blurred pages, a good image of the page can be found in the adjacent frame. If copyrighted materials were deleted, a target note will appear listing the pages in the adjacent frame.
3. When a map, drawing or chart, etc., is part of the material being photographed, a definite method of "sectioning" the material has been followed. It is customary to begin filming at the upper left hand corner of a large sheet and to continue from left to right in equal sections with small overlaps. If necessary, sectioning is continued again—beginning below the first row and continuing on until complete.
4. For illustrations that cannot be satisfactorily reproduced by xerographic means, photographic prints can be purchased at additional cost and inserted into your xerographic copy. These prints are available upon request from the Dissertations Customer Services Department.
5. Some pages in any document may have indistinct print. In all cases the best available copy has been filmed.

**University
Microfilms
International**
300 N. Zeeb Road
Ann Arbor, MI 48106

Tobin, Kathleen Marie

**THE DESIGN AND CONSTRUCTION OF A MICROPROCESSOR-COMPUTER
CONTROLLED RAPID SCANNING FIBER OPTIC SPECTROPHOTOMETER**

Western Michigan University

M.A. 1985

**University
Microfilms
International** 300 N. Zeeb Road, Ann Arbor, MI 48106

Copyright 1985

by

Tobin, Kathleen Marie

All Rights Reserved

**Copyright by
Kathleen Marie Tobin
1985**

TABLE OF CONTENTS

ACKNOWLEDGEMENTS	ii
LIST OF TABLES.....	vi
LIST OF FIGURES.....	vii
CHAPTER	
I. INTRODUCTION	1
Historical	1
Early Visual Instrumentation.....	1
Filter Photometers	1
Photometric Scanning Spectrophotometers..	2
Rapid Scanning Spectrophotometers.....	3
Microprocessors in Spectrophotometers.....	3
Fiber Optics.....	4
Physics.....	4
Applications.....	13
II. RAPID SCAN FIBER OPTIC SPECTROPHOTOMETERS.....	15
Advantages.....	15
Fiber Optic Spectrometers.....	15
Rapid Scanning Spectrophotometers.....	15
Design and Construction.....	16
Design Principles.....	16
Optics.....	16
Electronics.....	18
Optical System.....	25

Table of Contents - Continued

CHAPTER

	Microprocessor System.....	27
	Hardware.....	27
	Software.....	27
	Block Diagram.....	29
	Apple/Isaac System.....	29
	Hardware.....	29
	Software.....	31
	Block Diagram.....	32
III.	RAPID SCANNING FIBER OPTICS SPECTROPHOTOMETER APPLICATIONS.....	35
	Introduction.....	35
	Data.....	38
	Microprocessor System.....	38
	Apple/ISAAC System.....	38
	Absorbance and Derivative Spectra...	38
	Kinetics Photometer.....	43
	Photometric Titrator.....	45
	Acid-Base Titrator.....	48
	Complexometric Titrations.....	49
	Fluorometer.....	52
	Nephelometry and Turbidimetry.....	55
	Emission Photometer.....	56
	Conclusions.....	59
	Microprocessor System.....	59
	Apple/Isaac System.....	59

Table of Contents - Continued

APPENDICES

A. Rofin Monochromator.....	61
B. Heath Hardware.....	64
C. Microprocessor Software and Flowcharts.....	70
D. Software and Flowcharts for the Apple/Isaac System.	81
REFERENCES.....	90

LIST OF TABLES

1.	Values of Transmittancy for Standard Copper Sulfate Solution.....	39
2.	Values of Transmittancy for Standard Cobalt Ammonium Sulfate.....	40
3.	Chromaticity Coordinates of Selected Samples.....	41
4.	Rate Constants for the Reaction Between Chromium (III) Ion and 0.1M Ethylenediaminetetracetic Acid at Various Temperatures and Hydrogen Ion Concentration...	47
5.	Determination of Neutralization Endpoints for 0.0100M HCl in 25.00 mL 0.0400M NH ₃ with Phenol Red Indicator	51
6.	Determination of Neutralization Endpoints for 0.0100 M HCl in 25.00 mL 0.0400M NH ₃ with Bromthymol Blue ..	51
7.	Endpoint Determination of 0.01241M EDTA vs. 10 mL 0.012586M CaCO ₃ Using 0.02% Calcein Indicator.....	53
8.	1,2-Dichlorofluorosein Endpoint Determination of 0.0100 M HCl vs. 25 mL 0.00400M NH ₃	53
9.	Nephelometric Endpoint Determination of 0.0100N AgNO ₃ vs. 20 mL 0.004995N KCN.....	57
10.	Turbidimetric Endpoint Determination of 0.0100N AgNO ₃ vs. 20.00 mL 0.004995N KCN.....	57

LIST OF FIGURES

1.	Limiting Meridional Ray in an Optical Fiber.....	7
2.	Relationship Between Mean Refractive Index and Wave-length.....	9
3.	Relative Transmittance Curve for a 6 ft. Fiber Bundle	10
4.	Relative Transmittance Curve for a Coated Arsenic Trisulfide Fiber Bundle.....	11
5.	Nominal Transmittance for a Mid-UV Fiber Optic Bundle	12
6.	Typical Diode Array Arrangement.....	17
7.	Scanning Monochromator System Schematic.....	19
8.	Types of A/D Converters.....	21
9.	Types of D/A Converters.....	23
10.	Fiber Optic Probe Tip/Mirror Holder.....	26
11.	Operational Amplifier Circuit.....	26
12.	Block Diagram of the Microprocessor Controlled Rapid Scanning Fiber Optic Spectrophotometer.....	30
13.	Block Diagram of the Apple/ISAAC Controlled Rapid Scanning Fiber Optic Spectrophotometer.....	34
14.	Holmium Oxide Calibration Filter Standard Compared With Spectrum Obtained From Fiber Optic Spectrophotometer.....	36
15.	Didymium Calibration Filter Spectrum Compared to Spectrum Obtained From Fiber Optic Spectrophotometer.	37
16.	Comparison of 0.001M KMnO_4 Spectra From Beckman Model DU-6 Spectrophotometer and the Computer Controlled Rapid Scanning Fiber Optics Spectrophotometer.	42
17.	First and Second Order Derivatives of 0.001M KMnO_4 Spectra Comparison Between Fiber Optic Instrument and Beckman Model DU-6.....	44

List of Figures - Continued

18.	Kinetic Plots for pH 5.02 for Cr(II) - EDTA Reaction.	46
19.	EndPoint Determination for 25 mL 0.040M NH ₃ vs. 0.010M HCl Using Phenol Red Indicator.....	50
20.	Emission Spectrum of Tungsten Source Showing An Uncor- rected Detector Response.....	58
21.	Emission Spectrum of Sodium Vapor Source Showing an Uncorrected Detector Response.....	58

CHAPTER I

INTRODUCTION

Historical

Early Visual Instrumentation

Spectroscopy is the oldest of the optical methods of analysis, originating in 1666 with Isaac Newton's discovery that white light can be dispersed into its component parts with the subsequent discovery of spectra and the investigation of dispersion (1). The measurement of the absorption of visible radiation provides a convenient means for the analysis of numerous inorganic and organic species. The human eye was the receptor in the first types of these measurements with the accuracy depending upon the observer (2). The intensity relationship of the spectral lines was established by comparison to a series of standards. Examples of early instrumentation involving these types of intensity measurements are Hehner tubes, Nessler tubes and the DuBoscq colorimeter (3).

Filter Photometers

Filter photometers, such as the Klett-Summerson filter photometer, provide a simple relatively inexpensive tool for absorption analyses. The filter choice for a given analyte plays an important

role in determining the sensitivity of the measurement. The filter color should be complementary to the color of the solution as well as exhibiting its maximum transmittance in the wavelength region of maximum analyte absorbance.

Double beam instruments have been developed for photometer systems which compensate for source instability. The Spekker photometer employs a beam splitter to send the light through both the sample and the reference with the emerging light falling on a photographic plate as two spots (4). These spots are then compared to a previously prepared plate so that the darkened areas may be matched to obtain relative absorbances.

Photometric Scanning Spectrophotometers

The first commercial photoelectric spectrophotometer was designed by Hardy over fifty years ago (5). It was developed by the General Electric Company and used primarily in the visible region. A manual photoelectric spectrophotometer was designed in 1941 by Cary and Beckman (5). This instrument required the manual recording of the absorbance values for each sample at a given wavelength. Automated absorbance measurements came about later that year when Beckman modified the instrument to plot an absorbance value for each wavelength on the graph. It was not until the late 1950's that a continuous output of absorbance vs. wavelength became available (6).

Rapid Scanning Spectrophotometers

Due to the sluggishness of mechanical wavelength drives, finite response time of detectors and their associated measuring circuits, the process of scanning and recording the spectrum over the full ultraviolet-visible wavelength range (200-800 nm) took an appreciable length of time, frequently varying from one to ten minutes. The replacement of the photomultiplier tube with a photodiode array such as in the Hewlett-Packard model 8450-A spectrophotometer, resulted in the simplification of the complete optical system (7). Another alternative to the photodiode array is demonstrated with the Rofin Model 6011 Optical Spectrum Analyzer which utilizes a continuously rotated grating to separate the incoming light into its component wavelengths (8).

Microprocessors in Spectrophotometers

The incorporation of microprocessors in spectrophotometers has revolutionized the precise control of instruments and the collection of experimental data. More recently the microprocessor has been used to perform logic functions such as spectral comparisons, scale expansions and contractions, and differentiation virtually instantaneously (9). These functions have been accomplished largely by interfacing a microprocessor to an instrument, such as has been done with the Perkin-Elmer Model 3500 Data Station (10). However, interfacing and accompanying software are usually quite expensive if done on an instrument by instrument basis.

Modifications of the spectrophotometer to better adapt it to the microprocessor have also been made. The DU-7 ultraviolet-visible spectrophotometer (Beckman Instruments, Inc.) uses a single-beam monochromator with a specially stabilized light source and detector. The instrument has a microcomputer which stores reference data, complete wavelength scans, and complete analytical methods; computes expanded scales, derivative, or log information; picks peaks; subtracts or divides absorbance values at selected wavelengths; and performs many functions that formerly required the use of a data station (11). Other microcomputer controlled spectrophotometers include titrator and rapid scanning reflectance systems (12,13).

Fiber Optics

Physics

A smooth transparent cylinder, such as a glass rod, will transmit light by multiple internal reflections along its walls. This also occurs when the rod is reduced to a small diameter as in a fiber (14). This principle is termed total internal reflection and the conditions exist at any smooth interface between two transparent materials where the refractive index of the outer medium is less than that of the inner medium, such as that between glass and air. The presence of contamination, the condition of fibers touching one another or minute defects at the surface of the interface, interferes with the total internal reflection by absorbing or scattering

a fraction of the light. In most optical components, these losses are not serious since only a limited number of internal reflections occur. However, these losses become very serious in fiber optics since each light ray may undergo hundreds or thousands of reflections as it passes through the fiber (15).

When the fibers are brought into contact with one another the leakage of light from one fiber to an adjacent fiber can occur. This is called optical crosstalk and arises due to the penetration of the electromagnetic field into a rarer medium during total internal reflection. Attempts to prevent the leakage include coating the fibers with a highly reflecting material such as silver, but the small amount of absorption by the metal with every reflection destroys the transmission efficiency of the fibers. The use of a transparent dielectric coating make it possible to minimize the leakage while maintaining a high transmission efficiency. A transparent glass coating or cladding of low refractive index over the higher refractive index fiber is one way of accomplishing this (16). This also permits tightly packing of the cladded fibers into bundles with each fiber conducting light independently.

Optical fibers are basically waveguides for electromagnetic radiation at optical frequencies but many of their properties can be expressed in terms of geometric optics. The numerical aperature of optical fibers is a measure of the light gathering power as in the case of simple lens optics and is one of the principal properties of

a fiber or a bundle of fibers. Figure 1 shows two types of cylindrical fibers, (a) uncoated and (b) coated with light entering the fiber and reflecting from the innermost interface at the critical angle I_c . The critical angle is the largest angle at which an entering ray can be reflected totally thus determining the maximum angle from the meridional ray which can be accepted for transmission along the fiber. The same condition exists at the other end of the fiber with the emerging light (17).

The numerical aperture, N.A., of a fiber optic element can be derived from Snell's Law and may be calculated from Equation 1:

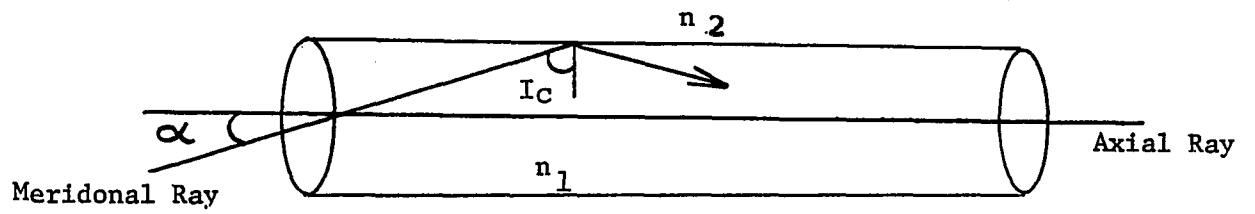
$$\text{N.A.} = n_3 \sin \theta = (n_1^2 - n_2^2)^{1/2}$$

where n_1 , n_2 and n_3 are the refractive indices for the core material, the cladding material and the medium surrounding the incident or emergent ray, respectively. From the N.A. one may calculate the f/Number by Equation 2:

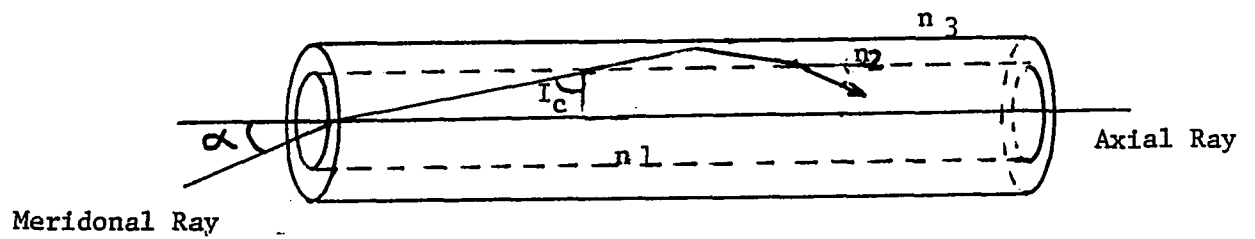
$$\text{f/Number} = \text{N.A.}/2$$

As the size of the fiber is reduced the limiting angle is not as sharply defined as the formula implies. Factors tending to diffuse the acceptance angle are diffraction, striae and surface irregularities on the fiber walls. As a result, it is best to assume the effective N.A. to be somewhat less than the calculated N.A.

In glass-coated glass-core fibers there is a fairly large range of refractive indices to choose from. By selecting various pairs of glasses it is possible to obtain almost any value of numerical aperture up to about 1.2 for visible studies and down to as small



a. Uncoated Fiber



b. Coated Fiber

Figure 1. Limiting Meridional Ray in an Optical Fiber.

an amount as desired, limited by the variations in the refractive index in the materials themselves (18). In choosing these glass pairs, their mutual compatability must also be considered such as: chemical and thermal compatability, stability, light attenuation and cost. In general the higher the refractive index of the core, the higher the N.A., but the lower the transmittance in the blue region of the spectrum. The relationship between refractive index and wavelength is illustrated in Figure 2.

The glasses normally used in fiber optics transmit light in the visible region, 400-1300 nm. Figure 3 shows the nominal transmission characteristics for a glass core commonly used in fiber optics (19). Glass strongly attenuates electromagnetic radiation beyond 1300 nm. An arsenic trisulfide glass core ($n_D = 2.47$) and a modified arsenic sulfide cladding ($n_D = 2.416$) is available for infrared transmission up to seven microns. Its transmission characteristics are shown in Figure 4 (20). For wavelengths below 350 nm where again glass attenuates severely, ultraviolet transparent materials are necessary for the core and cladding materials. Due to chemical and physical difficulties associated with most of these materials, quartz appears to be the best core material available at this time. Figure 5 illustrates the nominal transmission characteristics for a mid-ultraviolet fiber optics bundle (21).

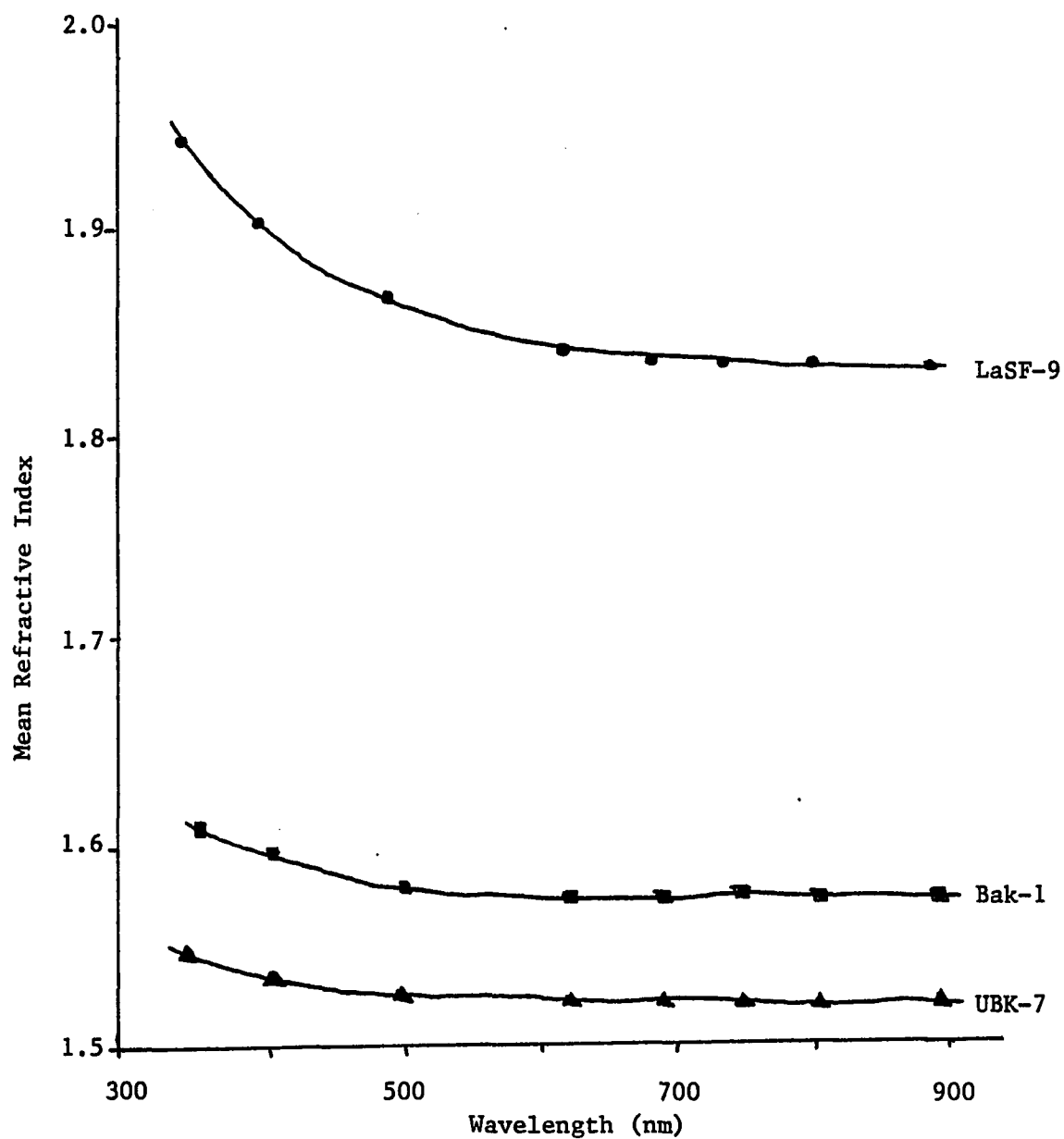


Figure 2. Relationship Between Mean Refractive Index and Wavelength

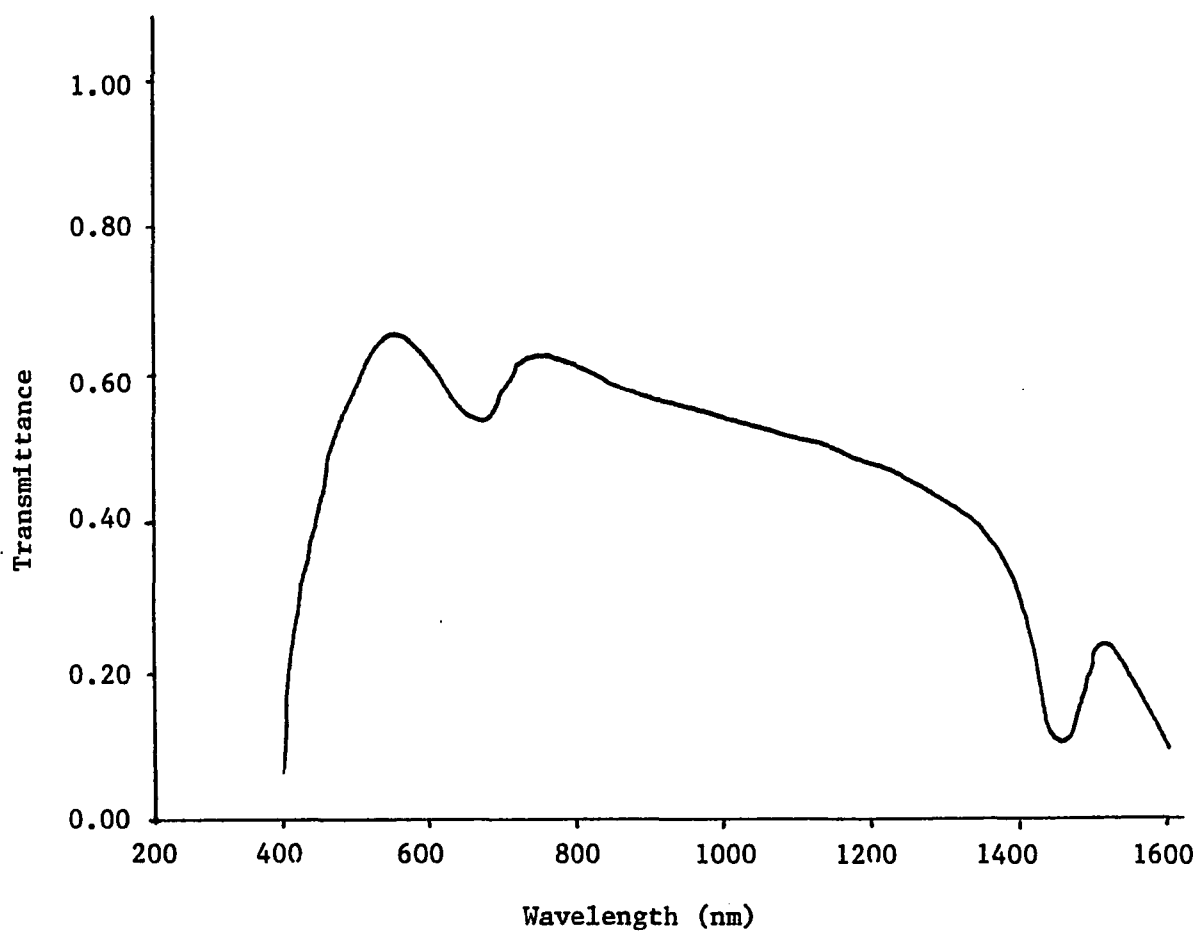


Figure 3. Relative Transmittance Curve of a 6 ft. Fiber Bundle

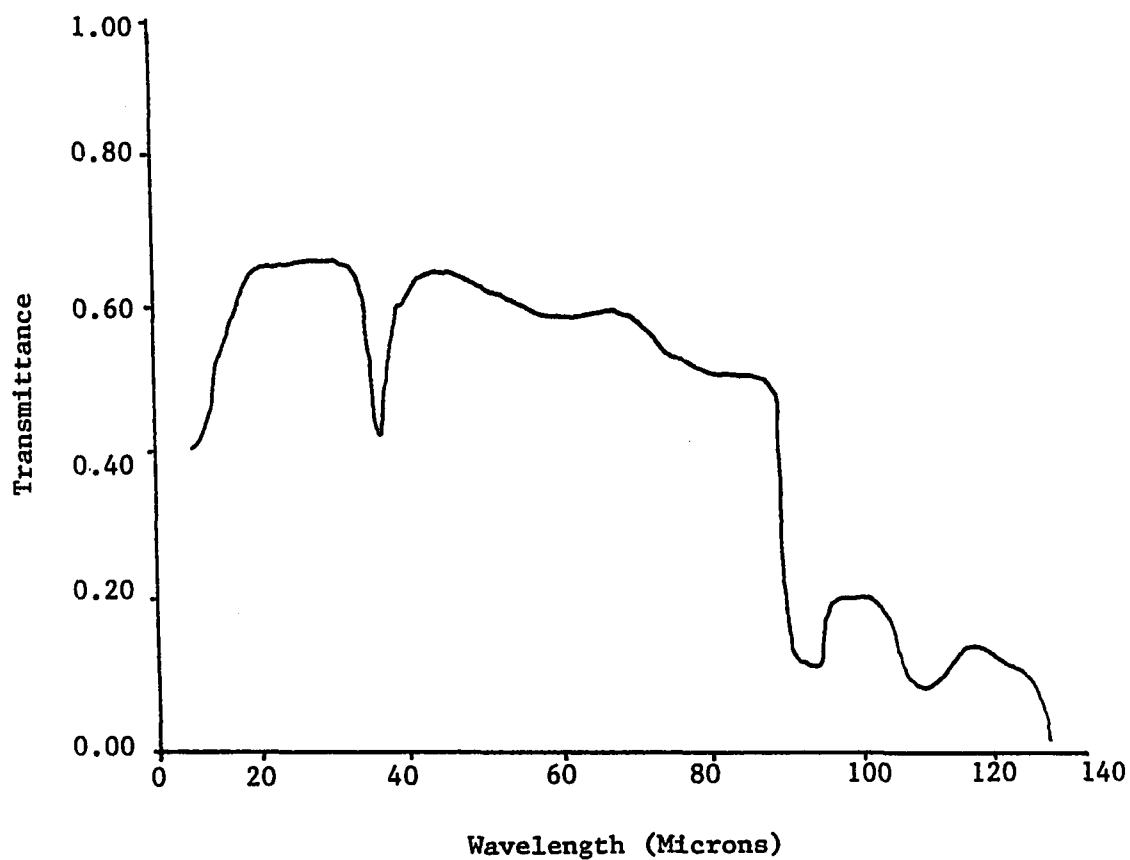


Figure 4. Relative Transmittance Curve for a Coated Arsenic Trisulfide Fiber Bundle

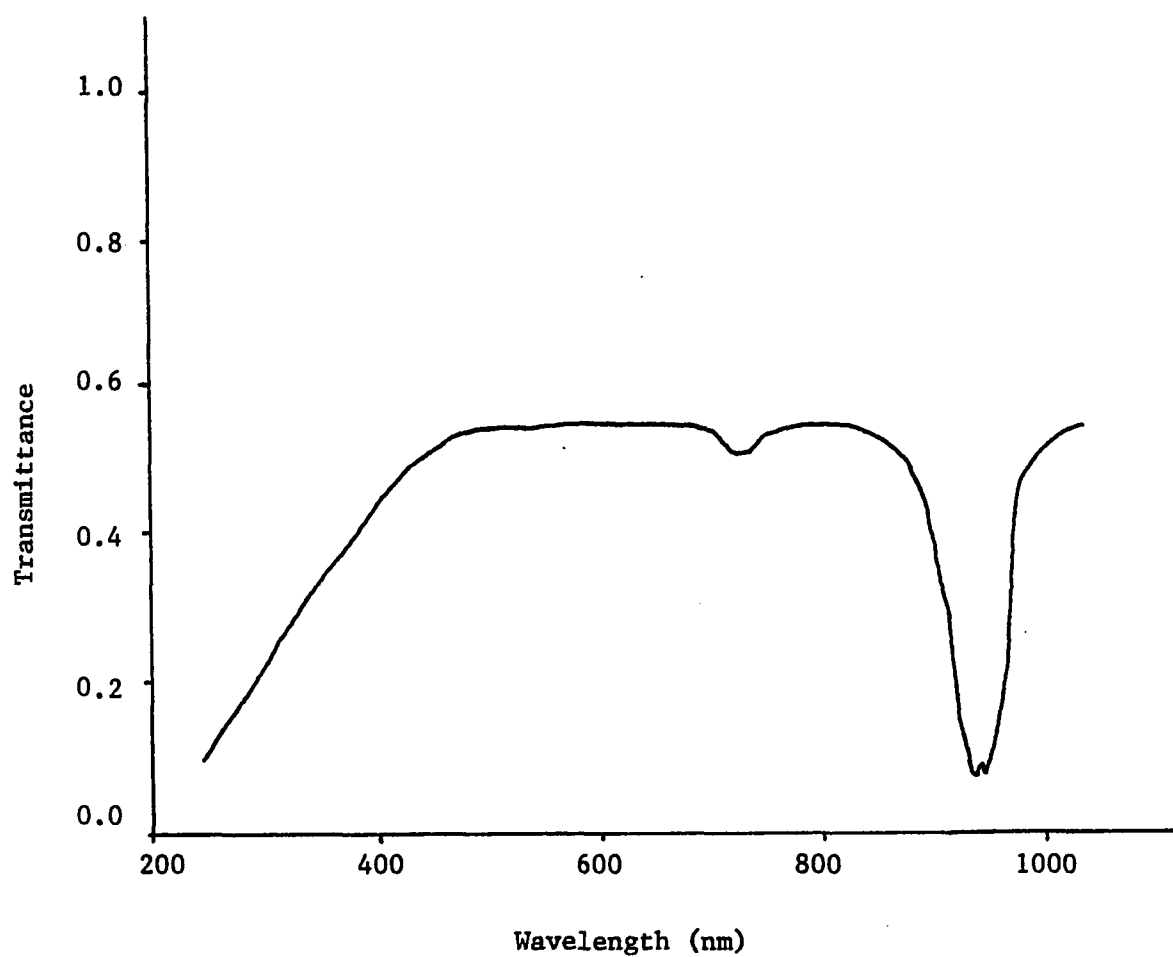


Figure 5. Nominal Transmittance for a Mid-UV Fiber Optic Bundle.

Applications

Fiber optics have been useful in the solution of many unique optical problems. One of the earlier applications was their use for the reading of computer tapes and cards (22). The medical field has also made significant use of fiber optics; for example "cold light" can be obtained over a surgeons operating table by piping it from a source in another room. This same type of illumination is also advantageous on microscope stages. The development for viewing the alimentary canal and bronchial tubes as well as the heart and viewing of fetuses are other advances in the medical field due to fiber optics. The use of fiberscopes in the automotive industry makes it possible to examine the inner workings of machines without following conventional methods (24).

Many components of conventional spectroscopic systems are being replaced by fiber optics. The optical fibers can be used for scanning thin-layer chromatograms and measuring their diffuse reflectance. In this type of system a second fiber bundle can be used to monitor the blank space adjacent to the spots for background variation corrections. This double beam operation also used in other analytical techniques such as fluorimetry, electrophoresis and monitoring particulate and thin films during vacuum deposition (25). Optical fibers are also used for the determination of colorimetric end points with the fiber optic bundle eliminating the need for the sample cell. A two bundle design using one fiber bundle to conduct light to the sample and the other to carry light that has passed

through the solution to a photocell has been reported (26,27). Another adaptation for colorimeter usage is the probe colorimeter where half the fiber bundle transmits light into the test solution and the light is returned to the instrument by the other half after being reflected by a mirror at a fixed distance from the end of the fiber optic bundle (28-30).

CHAPTER II

RAPID SCAN FIBER OPTIC SPECTROPHOTOMETERS

Advantages

Fiber Optic Spectrometers

Conventional spectrophotometers require the transfer of sample to a cuvette for obtaining spectra. A fiber optic spectrometer provides for direct placement of the fiber optic probe into the sample, thus allowing the measurement of absorbance in situ. The fiber optic systems offer other advantages over the traditional cuvette system such as minimizing thermal, vibrational and other environmental factors which might affect the absorbing species and its measurement. The small size of the optical bundles can also allow measurement of very small samples and in some instances single fibers for in vivo analysis. The flexibility of the fibers permits remote monitoring of highly radioactive samples as well as samples over wide ranges of temperature and pressure.

Rapid Scanning Spectrophotometers

Rapid scanning spectrophotometers permit the monitoring of fast reactions through repetitive scanning. High scan speeds allow for essentially simultaneous wavelength monitoring. A rapid scanning

system in conjunction with a microprocessor or computer offers other advantages such as time averaging in order to accomodate extensive data handling operations when low signal-to-noise ratios are encountered in single beam systems while still retaining high precision, dynamic range and resolution.

The effect of coupling a rapid scanning spectrophotometer with fiber optics combines these characteristics to provide an extremely versatile system. Additionally such an instrument can be used to determine reflectance spectra, endpoints in photometric, turbidimetric, or nephelometric titrations, kinetic studies, and fluorescence monitoring. The application of microprocessor or computer control and data manipulation makes spectral derivatization on feasible, thus enhancing minor spectral features in the spectra.

Design and Construction

Design Principles

Optics

There are two effect two systems for obtaining rapid spectral scanning: the diode array detector and the scanning grating monochromator. A typical diode array consists of a row of silicon photodiodes, each with an associated storage capacitor for integration of the photocurrent and a multiplexer switch for readout (31). This is illustrated in Figure 6. The light incident on the sensing area permits the passage of charge which is collected and

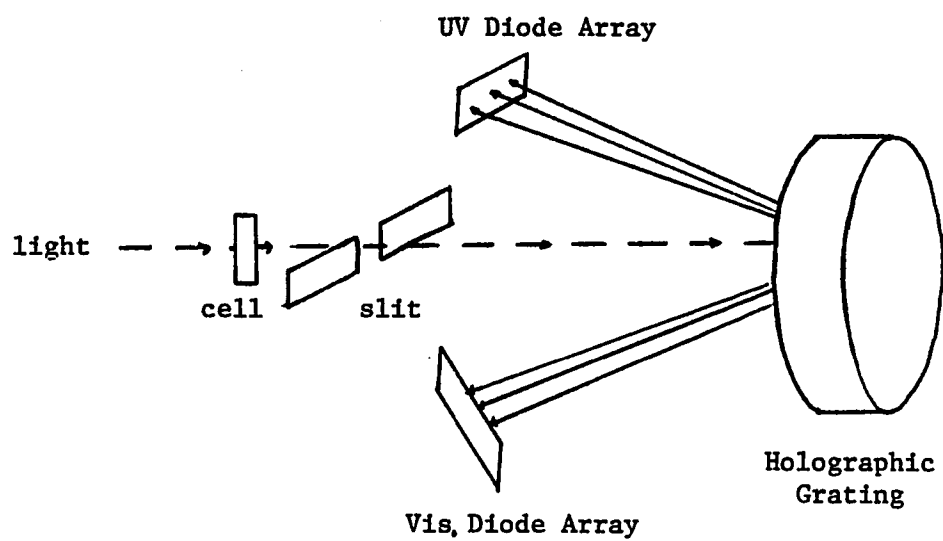


Figure 6. Typical Diode Array Arrangement.

stored during the integration period. The accumulated charges are sequentially switched for output. The photocurrent is the product of the diode responsivity and the light intensity.

The scanning monochromator usually consists of a single pass Czerny-Turner grating with a precision lead screw sine-bar assembly. This sine-bar assembly drives the diffraction grating and provides accurate wavelength selection and resettability (32). A typical scanning monochromator system is shown in Figure 7. These grating monochromators are relatively inexpensive and have good wavelength accuracy.

Electronics

The purpose of an interface is to accept the experimental data and/or parameters from an instrument and transmit them to the computer in a compatible format as well as providing a means for reverse communications to allow the computer to control the instrument. All interfaces consist of hardware between the instrument and computer or in the instrument itself. The proportion of interfacing functions that are provided vary by hardware and software with each type of interface. They may also vary with the amount of design interfacing that the user must do.

Most instruments provide an analog output. The purpose of an analog interface is to convert the analog signal to a binary form that can be read by the digital computer. Analog to digital (A/D) converters are characterized by their resolution, accuracy, conversion time (maximum throughput) and their dynamic range.

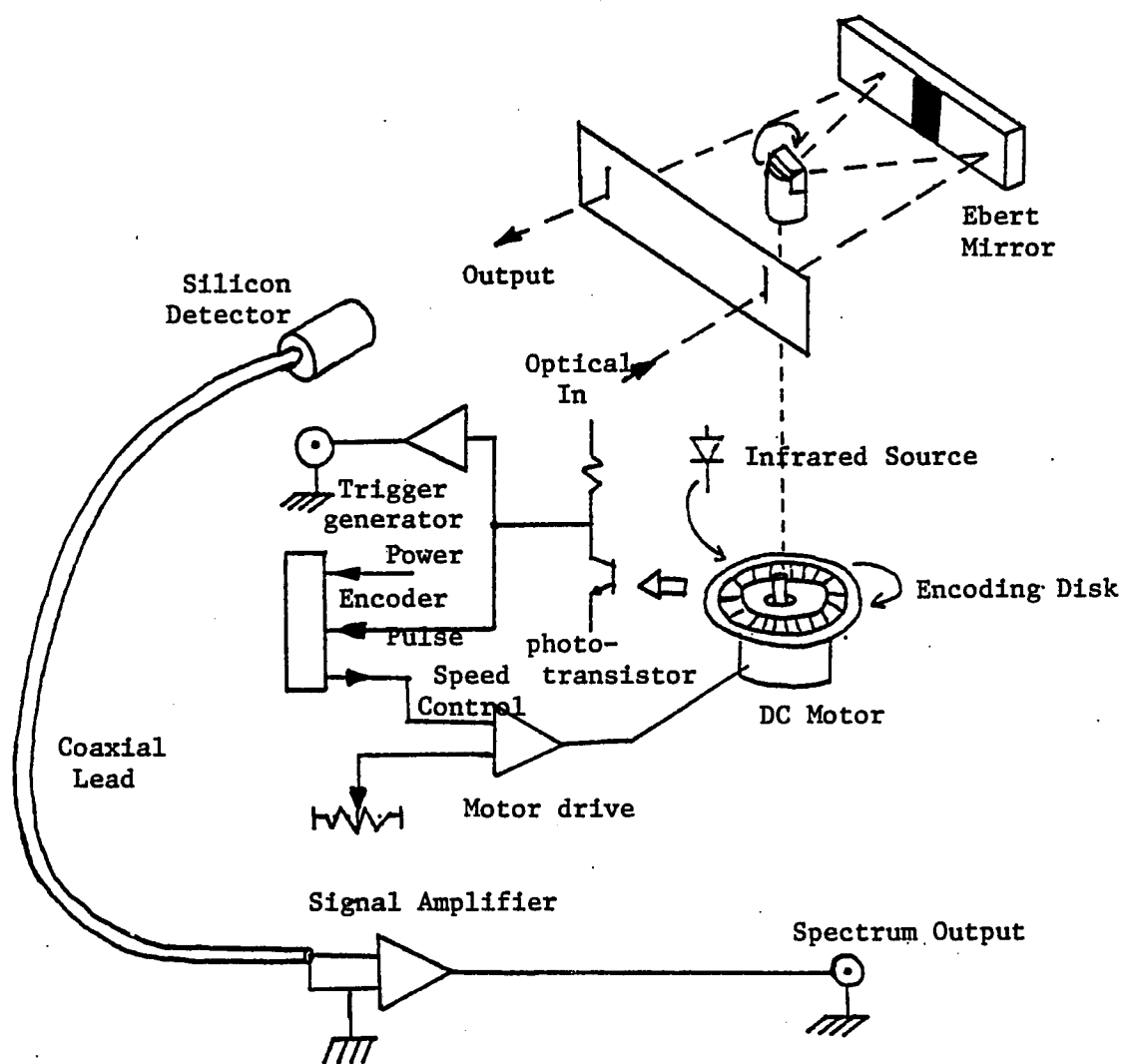


Figure 7. Scanning Monochromator System Schematic.

There are two types of effective A/D converters dominating the field. They are the shift programmed successive approximation and the dual slope integration types. In a dual slope integrating A/D converter, Figure 8a, the conversion is accomplished by first charging an integrating capacitor and then discharging it back to zero. The analog signal is used to charge the capacitor for a fixed time interval, determined by the converter's clock rate and digital counter capacity. Then after resetting the counter, an internal standard reference voltage is substituted for the input signal and the capacitor is discharged back to zero. The digital counter now registers a count, N_r , which is related to the internal standard voltage, E_r , the input signal voltage, E_s , and the counter value from the input signal, N_s , as shown in Equation 3:

$$N_r = (E_r/E_s) * N_s \quad (3)$$

Since E_s and N_s are fixed by the circuit parameters, the state of the digital counter at the end of the conversion will be linearly proportional to E_r , and may thus be easily scaled and read directly (33).

Dual slope integrating A/D converters have many advantages over successive approximation converters. Since the input signal is integrated over precise time intervals, the conversion is effective in noisy electrical environments. These devices also have wide dynamic ranges and a lower cost for a given resolution and accuracy. However, since the capacitor is charged and discharged with each conversion, the conversion speed is significantly slower than that

of the successive approximation converter.

Shift programmed successive approximation converters, Figure 8b, operate by successively comparing the analog input with pre-programmed fractions of a reference signal generated by the computer through a digital to analog (D/A) converter. As each comparison is made, the output of the comparator is monitored and interpreted into greater than or less than states. The comparison process continues until the least significant bit (LSB) has been established as a binary one or zero, after which an end of conversion (EOC) signal indicates the output is ready for recording (34).

Speed is the inherent advantage of successive approximation A/D converters. Some of these devices are available with conversion times in the nanosecond range. In nearly all other respects, e.g. cost and reliability, the integrating A/D converters are superior to the successive approximation A/D converters.

The conversion of digital values to proportional analog values is a necessary task that results in digital operations being understood in the analog world. There are two types of digital to analog (D/A) converters commonly used, a constant resistance ladder network with branches switched in and out depending on the digital value to be converted, and a summing operational amplifier with binary weighted input resistances. Both types relate to the type of resistor network used in the circuit.

Weighted resistor D/A converters include a reference voltage source, a set of switches, a set of binary weighted resistors and an

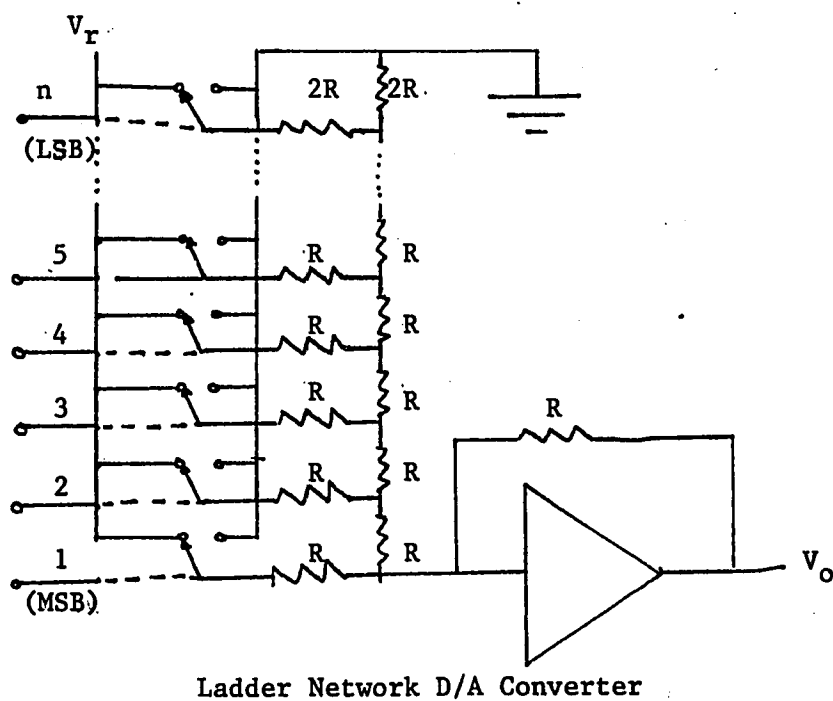
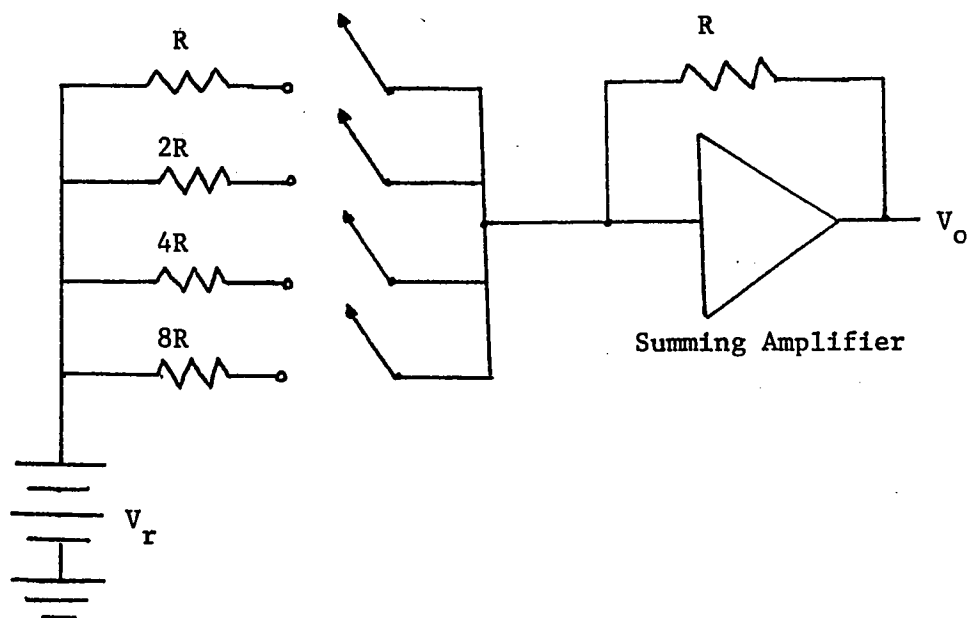


Figure 9. Types of D/A Converters

operational amplifier as illustrated in Figure 9a. Each bit of the binary input controls a switch, closing when the value is a binary one and opening for a binary zero. When the switch closes, the reference voltage crosses the weighted resistors in series and a current flows into the summing amplifier. When all the inputs are summed in the amplifier, the output voltage of the amplifier is proportional to the total current, i.e. the analog value of the digital input code.

The constant resistance ladder network converters also contain a reference voltage source, a set of switches, and an operational amplifier. Instead of a set of binary weighted resistors, they contain two resistors per bit. One is in series with the bit switch, the other is in the summing line. Figure 9b shows a simple four bit converter with this ladder network. The switches must switch a dc reference voltage with a high degree of accuracy, ideally having zero resistance when closed and infinite resistance when open. Output resistance is constant regardless of switch position, so that a fixed resistance load does not produce non-linearity errors. Each switch contributes its appropriately weighted component to the output voltage, resulting in a net output voltage that is proportional to the binary input (35).

The D/A converter, providing the microprocessor with the means for generating the analog signals, and the A/D converter, providing the means for measuring the analog signals, provide the basis of a conversion system. The peripheral interface adapter (PIA) allows

for communication between these external circuits and the microprocessor.

Optical System

The optical components used in the construction of both the microprocessor controlled and the computer controlled fiber optics rapid scanning spectrophotometer systems are the same. A Rofin Model 6000 monochromator was chosen for its low cost and highly versatile system of measuring and displaying spectra. The accuracy of the unit was improved with a Rofin Model 6001 wavelength marker (36). The Rofin silicon detector assembly was also used in conjunction with the internal transimpedance amplifier whose combination provides for a very high transimpedance gain with medium response speed. A complete description of the Rofin system may be found in Appendix A.

Light is transmitted through the sample with a four channel light guide. In operation, three-fourths of the fiber optic bundle transmits light into the sample region. The remaining fourth returns light to the monochromator unit where the light is dispersed into its component wavelengths before impinging on the silicon detector. Light may be returned to the light guide by the probe tip, Figure 10, on which is mounted a back surface aluminum oxide mirror at a specified distance from the end of the fiber optic bundle. This distance is half the effective path length since light travels through the sample twice, first to the mirror and then back to the

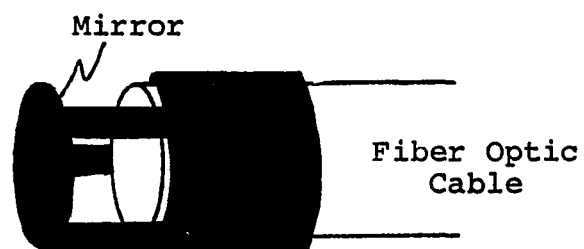


Figure 10. Fiber Optic Probe Tip/Mirror Holder.

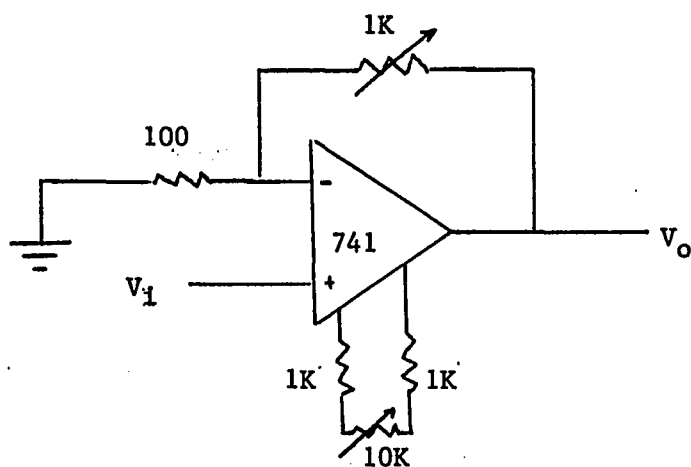


Figure 11. Operational Amplifier Circuit.

light guide. For reflectance studies, the probe tip is removed and the light guide placed on the sample. Thus reflected light is returned to the monochromator.

Microprocessor System

Hardware

The Heathkit Model ET-3400 Microcomputer Learning System is the practical, low cost microprocessor trainer used in the microprocessor controlled rapid scanning fiber optic system. The Heathkit Model ETA-3400 Memory I/O Accessory was used as an expansion unit, by adding Tiny BASIC and a terminal monitor, expansion RAM, and audio cassette program storage, the microprocessor was upgraded to a usable system. A serial I/O port provides communication to a Lear Siegler ADM 3A dumb terminal with a baud rate of 900. The Analog Devices ADC 1140 successive approximation A/D converter was used, providing high accuracy, 16 bit resolution, high stability, and a 35 us conversion time. The ADC 1140 was used with a Motorola MC 6821 "peripheral interface adapter" (PIA) for interfacing to the microprocessor. The Heathkit Microcomputer Learning System, Memory I/O Accessory and the PIA are described in more detail in Appendix B.

Software

Whatever the type of hardware interface, applications of software must be written for the computer to handle the data in a processible

form. Acquisition of data takes place when the instrument has data to send and the computer is prepared to accept it. Coordination of the data transfer is provided by the handshaking software of the computer. In general, the handshaking procedure involves the instrument sending a signal to the computer when it is ready to transmit data. If the computer is ready to accept the data, it sends an acknowledgement pulse on another line and then obtains the data sent by the instrument.

The microprocessor system monitors the wavelength marker, taking a reading every 10 nm for both baseline and sample data. To do this, the marker pulse voltage must be TTL compatible, 5 volts. Since the marker pulse is 1.5 volts for each nm an amplification is required. This is accomplished using an operational amplifier circuit as illustrated in Figure 11, where the output voltage is approximately three times that of the input voltage. The program for acquiring data uses the tenth count as a pulse for the A/D converter. As soon as the "end of count" (EOC) pulse reaches the PIA, the data are stored in memory. This continues until every wavelength value has been stored for baseline (P_0) and sample (P) spectra. Division of the analog values P/P_0 , results in transmittance values for each wavelength. The algorithm and program for data acquisition and transmittance calculation may be found in Appendix C.

The software in the microprocessor system also has two output options, one for binary coded decimal (BCD) representation of

transmittance and the other for output to the D/A converter for output to the oscilloscope and x-y recorder for hard copy of the spectra. The algorithms and programs for BCD conversion and output are also found in Appendix C. The data from the BCD conversion were entered into a chromaticity coordinate program on the Hewlett-Packard Model HP-85 computer. The program for this calculation may be found in Appendix C also.

Block Diagram

The complete microprocessor system is illustrated in Figure 12. The light is transmitted through three channels of a four channel optical cable to the probe tip. The remaining channel transmits light back to the monochromator. The signal generated by the detector is monitored by the ADC 1140 and the pulse from the wavelength marker by the amplifier/counter circuit. The signals from these components go to the PIA and then to the microprocessor for data storage and manipulation.

Apple/Isaac System

Hardware

Cyborg Corporation's integrated system for automated data acquisition and control (ISAAC) offers the capacity for enhanced performance with the integration of software and hardware components. The A/D and D/A converters employed are manufactured by

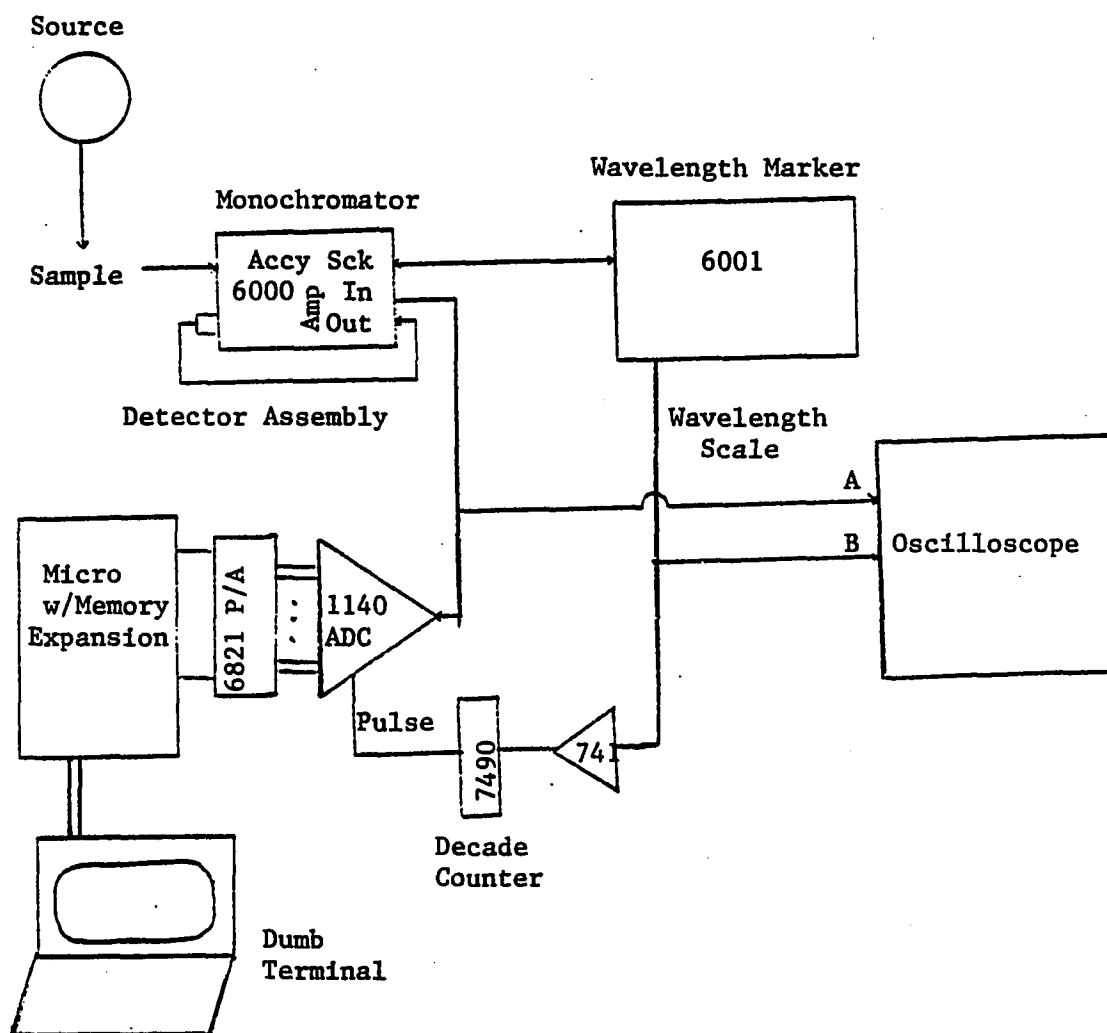


Figure 12. Block Diagram of the Microprocessor Controlled Rapid Scanning Fiber Optic Spectrophotometer.

Analog Devices. The analog inputs will accomodate several selectable voltage ranges, making for a full range of input voltages extending from 0.25 to 100 volts. Channel acquisition time is 100 us and conversion time is 25 us, for a total of 125 us per sample. However, using machine language greatly increases ISAAC's sampling rate without conversion time penalties.

The D/A outputs span the same voltage range as the A/D inputs. The binary inputs and outputs are available at separate terminals and can be treated as parallel 16-bit words, binary coded decimal data or as 32 separate channels. The Schmitt trigger input sub-assembly has four separate inputs with their threshold levels set by either front panel potentiometers or external references.

The 16-bit timer/counter has 1 ms resolution and is crystal controlled using the central processing unit's clock. The counter has one low level analog input and seven TTL level multiplexed clock inputs. The fiber optic scanning spectrophotometer system utilizes the A/D converters, the timer/counter and the Schmitt triggers of the ISAAC data acquisition system.

Software

Labsoft, an extended version of Applesoft BASIC, offers an additional forty new input/output, graphics and utility commands, tailoring Applesoft to the data acquisition task.

As in the microprocessor system the wavelength marker pulse acts as the initializing pulse. The pulse input calls an assembly based input/storage subroutine, TRANSIENT.OBJ. Labsoft, along with

the memory available in the Apple, allows for signal averaging, transmittance and absorbance calculations, derivatizations, kinetic calculations, and end point determinations. It also provides for a graphics option and data storage/retrieval to/from the disk.

The assembly based subroutine for input and storage, TRANSIENT.OBJ stores data values in a preprogrammed array for either baseline or sample data. The zero reading is then subtracted from each data point and the baseline scaling factor calculated for a maximum range. From these data values, transmittance or absorbance are calculated and then printed, plotted, deleted, stored or all options.

If the user desires derivatization, both transmittance and absorbance options are available for enhancing spectral sensitivity. Derivatives allow for precise wavelength determination of absorption maxima, improved resolution of a spectrum and also for quantitative determinations in multicomponent systems or in the presence of turbidity (29).

The program and flow charts for the Apple/ISAAC system, with all the options combined into a user friendly main program, may be found in Appendix D.

Block Diagram

The complete Apple/ISSAC system is illustrated in Figure 13. As in the microprocessor system, the light is transmitted to the probe tip by three channels of an optical guide with the fourth channel returning the light to the monochromator unit. The signals

from the detector and the wavelength marker are monitored by the ISAAC units A/D converter and the Schmitt trigger, respectively. The ISAAC unit then transfers the data to the Apple for manipulation and storage.

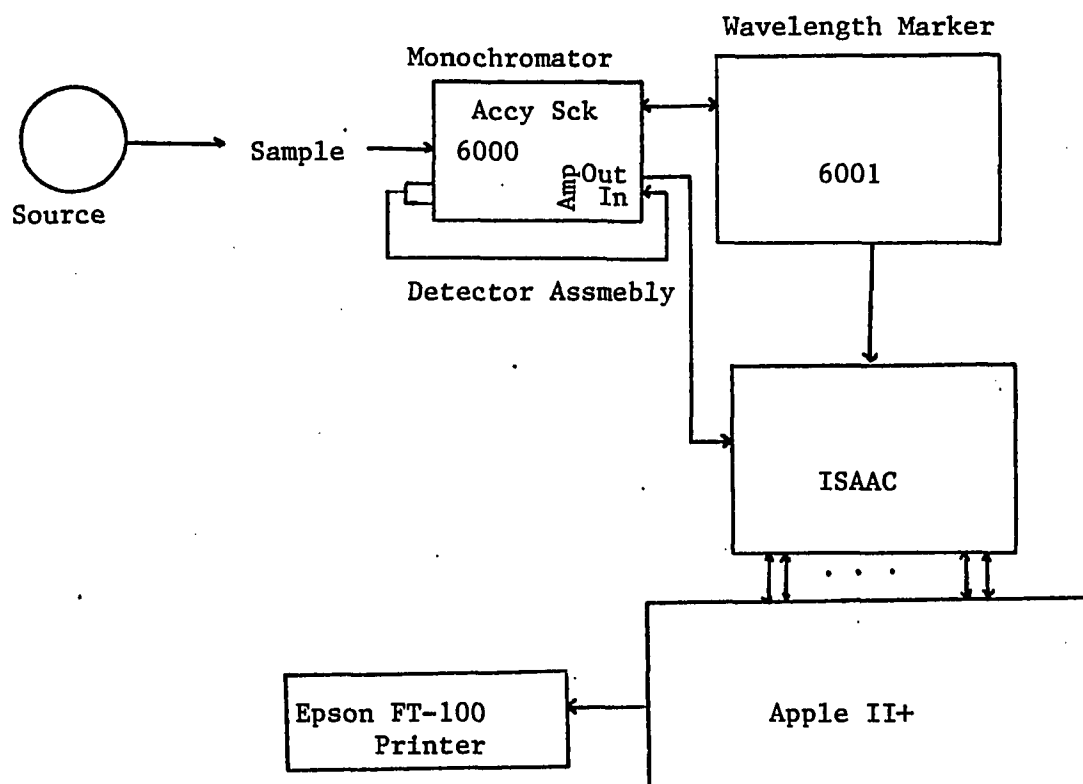


Figure 13. Block Diagram of the Apple/ISAAC Controlled Rapid Scanning Fiber Optic Spectrophotometer.

CHAPTER III

RAPID SCANNING FIBER OPTICS SPECTROPHOTOMETER APPLICATIONS

Introduction

The general applicability of the rapid scan fiber optic spectrophotometer was tested using established analytical procedures. The microprocessor system was used to obtain reflectance data, showing one of the many potential applications. The Apple/BASIC system was used to obtain transmittance and absorbance spectra, both with and without derivatives; to study a kinetic system at normal and elevated temperatures; and to determine end points for titrations with photometric, turbidimetric, and fluorescence end points. The precision of the Apple system was evaluated by the standard deviation from the mean of the data.

Since the intensity of the mercury vapor calibration lamp was lower than required for calibration purposes, a holmium oxide filter and a didymium glass calibration filter were used as tools for wavelength calibration. The holmium oxide filter, with sharper peaks, was used as a primary calibration source. A representative spectrum is shown in Figure 14. The didymium filter was then used to check the wavelength calibration, a typical spectrum is illustrated in Figure 15.

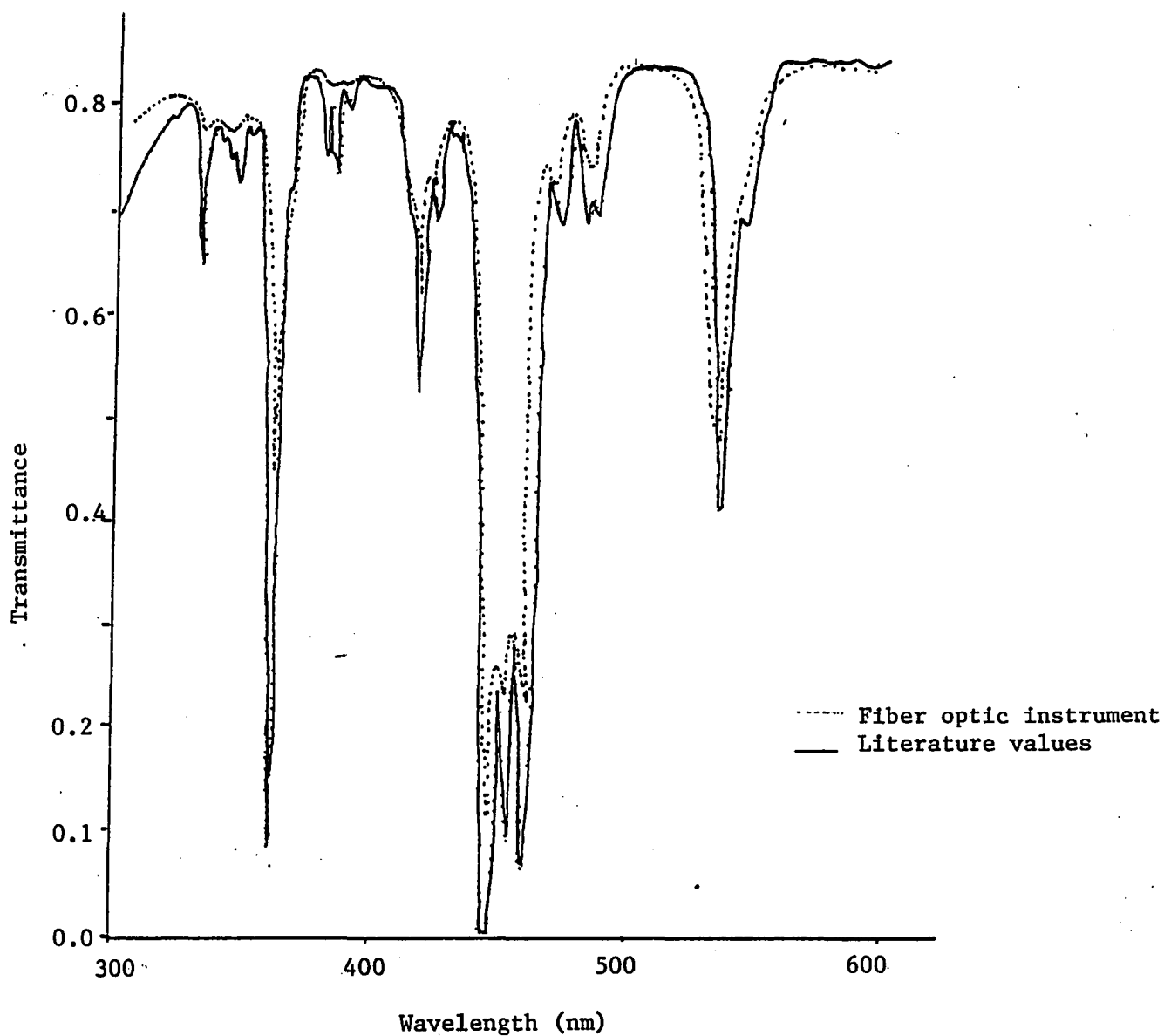


Figure 14. Holmium Oxide Calibration Filter Standard Compared With Spectrum Obtained From Fiber Optic Spectrophotometer.

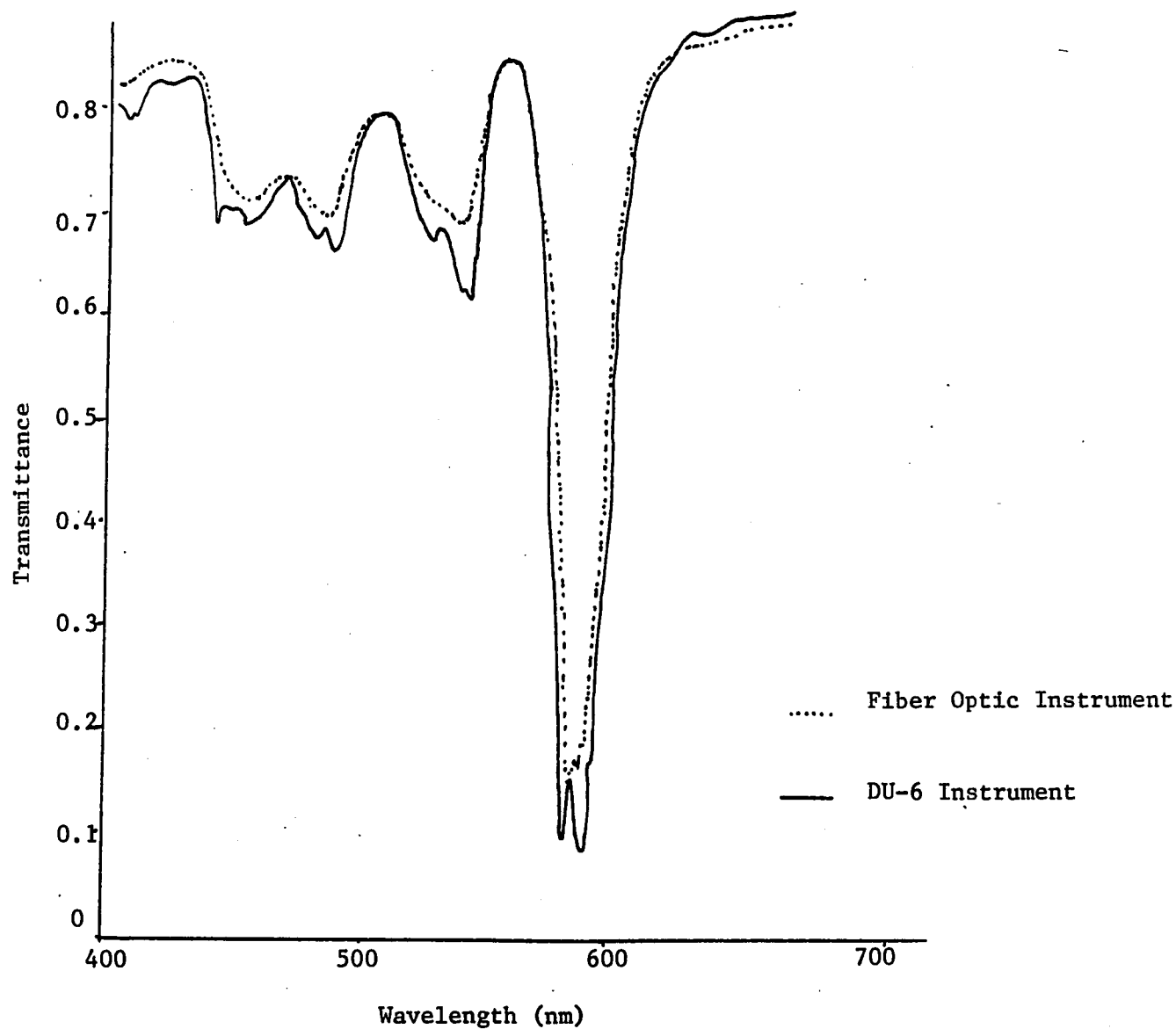


Figure 15. Didymium Calibration Filter Spectrum Compared to Spectrum Obtained From Fiber Optic Spectrophotometer.

The spectral transmittances and absorbances of aqueous solutions of copper sulfate and cobalt ammonium sulfate were used to check the photometric scale of the scanning spectrophotometer. The results may be found in Tables 1 and 2 for the solutions of copper sulfate and cobalt ammonium sulfate, respectively.

Data

Microprocessor System

The microprocessor controlled rapid scan fiber optics spectrophotometer was used to measure the reflectance spectra of colored paper with the results compared to the spectra obtained from a Bausch & Lomb Model Spectronic 20 with the reflectance attachment. Eight different samples were examined, the transmittancy values obtained and the chromaticity coordinates calculated. Table 3 shows the results of the reflectance study. The chromaticity coordinates obtained from the microprocessor system correlate well with those from the Spectronic 20.

Apple/ISAAC System

Absorbance and Derivative Spectra

To test the versatility of the spectrophotometric system, several studies were undertaken. Absorbance spectra of KMnO_4 were obtained with the Apple/ISAAC system and then compared to those obtained from a Beckman Model DU-6 spectrophotometer as shown in

Table 1

Values of Transmittancy for Standard Copper Sulfate Solution

Wavelength	T _{Lit}	T _{Exp}
350	.979	.942
60	.986	.951
70	.989	.963
80	.992	.971
90	.994	.972
400	.995	.972
10	.996	.973
20	.996	.975
30	.997	.977
40	.997	.977
450	.997	.980
60	.997	.980
70	.997	.980
80	.997	.979
90	.996	.979
500	.994	.975
10	.991	.970
20	.987	.969
30	.982	.965
40	.975	.963
550	.965	.956
60	.951	.939
70	.935	.929
80	.914	.910
90	.888	.889
600	.855	.856
10	.816	.815
20	.772	.773
30	.719	.720
40	.661	.660
650	.597	.595
60	.532	.535
70	.466	.465
80	.406	.404
90	.348	.351

Table 2

Values of Transmittancy for Standard Cobalt Ammonium Sulfate

Wavelength	T _{Lit}	T _{Exp}
350	.991	.974
60	.991	.974
70	.989	.970
80	.985	.966
90	.980	.964
400	.972	.959
10	.962	.945
20	.950	.937
30	.925	.908
40	.887	.867
450	.837	.828
60	.789	.772
70	.756	.749
80	.733	.729
90	.713	.711
500	.686	.664
10	.670	.647
20	.678	.674
30	.716	.712
40	.774	.734
550	.837	.803
60	.892	.868
70	.932	.899
80	.953	.907
90	.964	.912
600	.969	.920
10	.972	.922
20	.974	.929
30	.975	.930
40	.975	.930
650	.976	.946
60	.978	.949
70	.980	.942
80	.983	.945
90	.985	.947

Table 3

Chromaticity Coordinates of Selected Samples

Color	Spectronic 20			Fiber Optic		
	X	Y	Z	X	Y	Z
Pink (1)	.3592	.3026	.3382	.3591	.3029	.3389
Pink (2)	.3217	.3189	.3593	.3215	.3185	.3600
Orange (1)	.3888	.3637	.2455	.3882	.3639	.2479
Orange (2)	.3901	.3687	.2411	.3897	.3688	.2415
Green	.2920	.3555	.3525	.2922	.3549	.3592
Yellow	.3703	.4034	.2263	.3700	.4041	.2259
Blue-green	.2875	.3126	.3999	.2872	.3129	.3999
Off-white	.3206	.3286	.3508	.3189	.3297	.3514

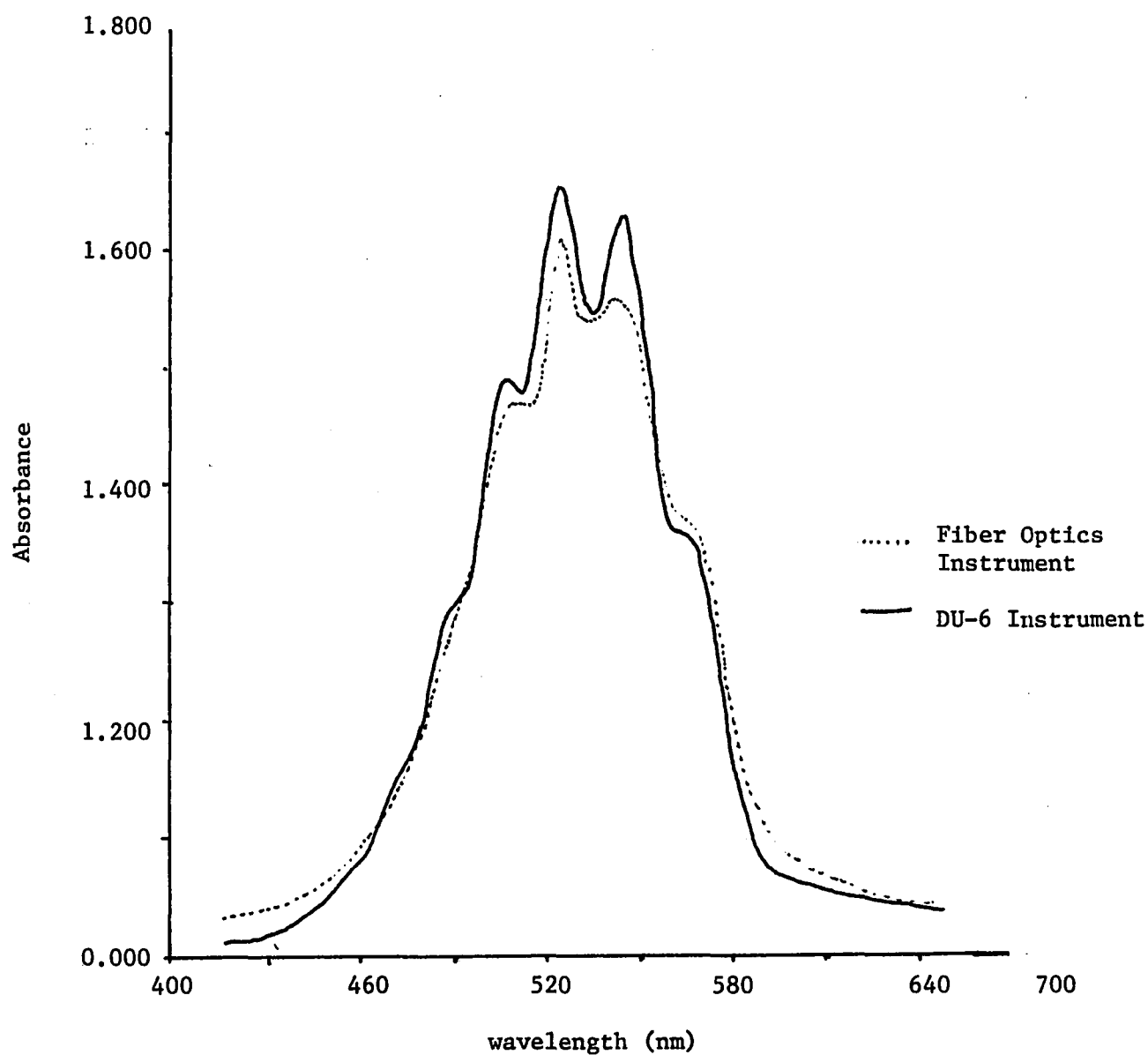
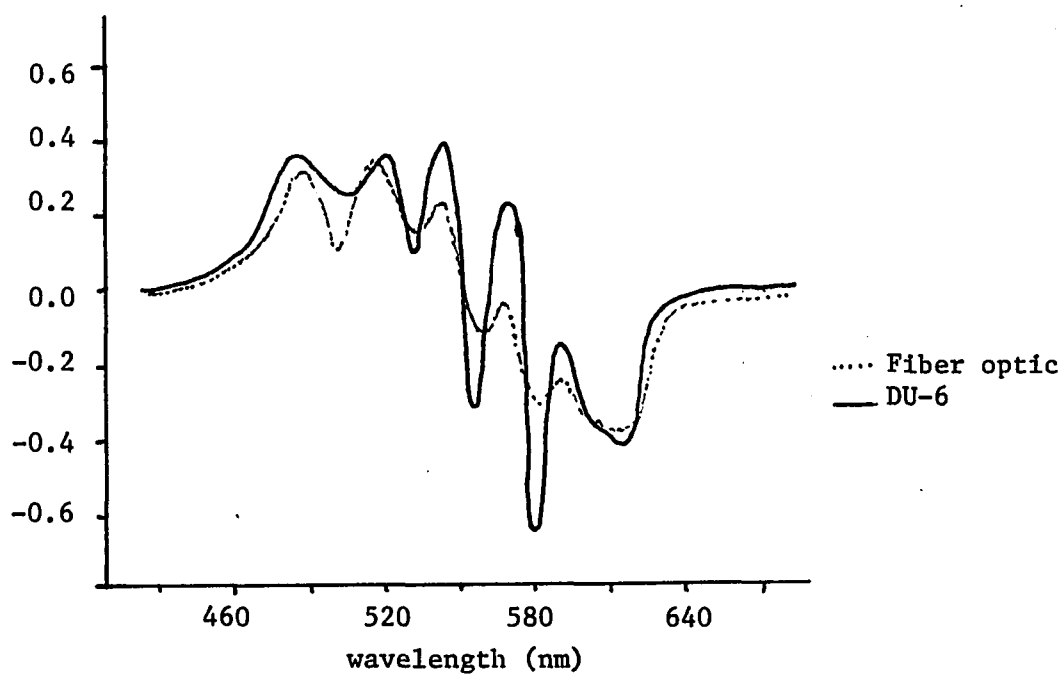


Figure 16. Comparison of 0.001M KMnO_4 Spectra From Beckman Model DU-6 Spectrophotometer and the Computer Controlled Rapid Scanning Fiber Optics Spectrophotometer.

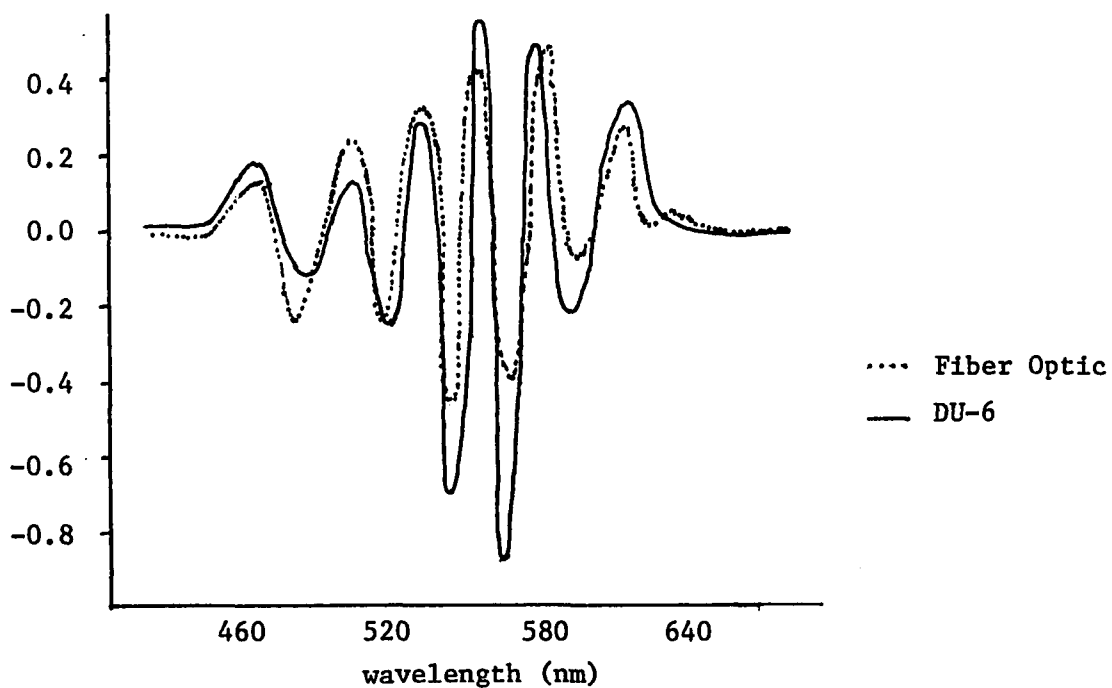
Figure 16. The higher resolution of the DU-6 was evident from the standard spectra of CuSO_4 and $\text{CoSO}_4(\text{NH}_4)\text{SO}_4$ solutions, nevertheless the general shape of the curve is quite similar. Once the data is obtained and stored, other massaging operations can be employed using the computer system, i.e. data smoothing, derivatives or volume corrections for absorbance or transmittance measurements. To illustrate the derivative technique, the first and second derivatives of KMnO_4 spectra from the Apple/ISAAC system compared to the spectra from the Beckman Model DU-6 are shown in Figure 17. Since the Beckman system has little available memory for data storage, each spectrum obtained required the sample to be rescanned with the instrument in the corresponding derivative mode. Thus the Apple/ISAAC system is much faster than the DU-6 in these applications, but at the expense of some resolution.

Kinetics Photometer

The absorption spectra of both the blue and the violet forms of ethylenediaminetetraacetic (EDTA) complex with chromium(III) ion and the dependence of these forms on temperature and on hydrogen ion concentration were used to illustrate the kinetics applications of the system (37,38). A 0.0528M Cr(III) solution was prepared by dissolving 14.612 g $\text{Cr}(\text{NO}_3)_3$ in 500.0 mL of doubly distilled water. 5.0 mL of the Cr(III) solution was then added to 2.00 g EDTA in solution, enough sodium hydroxide or nitric acid added to bring the pH to 5.02 or 5.50, and the reaction followed at both 30.0°C and 22.0°C in constant temperature baths. The ionic strength was not



First Derivative of 0.001M KMnO_4 Spectra



Second Derivative of 0.001M KMnO_4 Spectra

Figure 17. First and Second Order Derivatives of 0.001M KMnO_4 Spectra Comparison Between Fiber Optic Instrument and Beckman Model DU-6

controlled since accurate rate constant determination was not the objective of the experiment. Data were taken every thirty minutes over a three hour time period for pH 5.02 and every ten minutes over a one hour time period for pH 5.50. At the end of the time period, the solutions were heated at 100°C for ten minutes in order to allow the reaction to reach completion and then cooled, thus obtaining an absorbance value for the unreacted chromium(III) as shown in Equation 4:

$$A_{\text{Cr(III)}} = A - A_t \quad (4)$$

The apparent rate constant is obtained by plotting $\log (A - A_t)$ versus time as shown in Figure 18 for the pH 5.02 kinetic system. Table 4 shows the experimentally obtained rate constants for this series of measurements. The data indicates that pseudo first order kinetics are followed when the pH is held constant.

Photometric Titrator

Spectrophotometric measurements may be employed in locating the equivalence point of a titration. A typical spectrophotometric titration curve consists of a plot of absorbance versus the volume of titrant added. Providing the correct conditions have been chosen, the plot consists of two straight line segments of different slope with the equivalence point taken as the intersection resulting from the extrapolation of the straight line segments. By placing the light probe into the titration vessel, the absorbance data are collected as the titrant is added. Indirect titrations employ the addition of indicator whose absorbance is observed as a function of

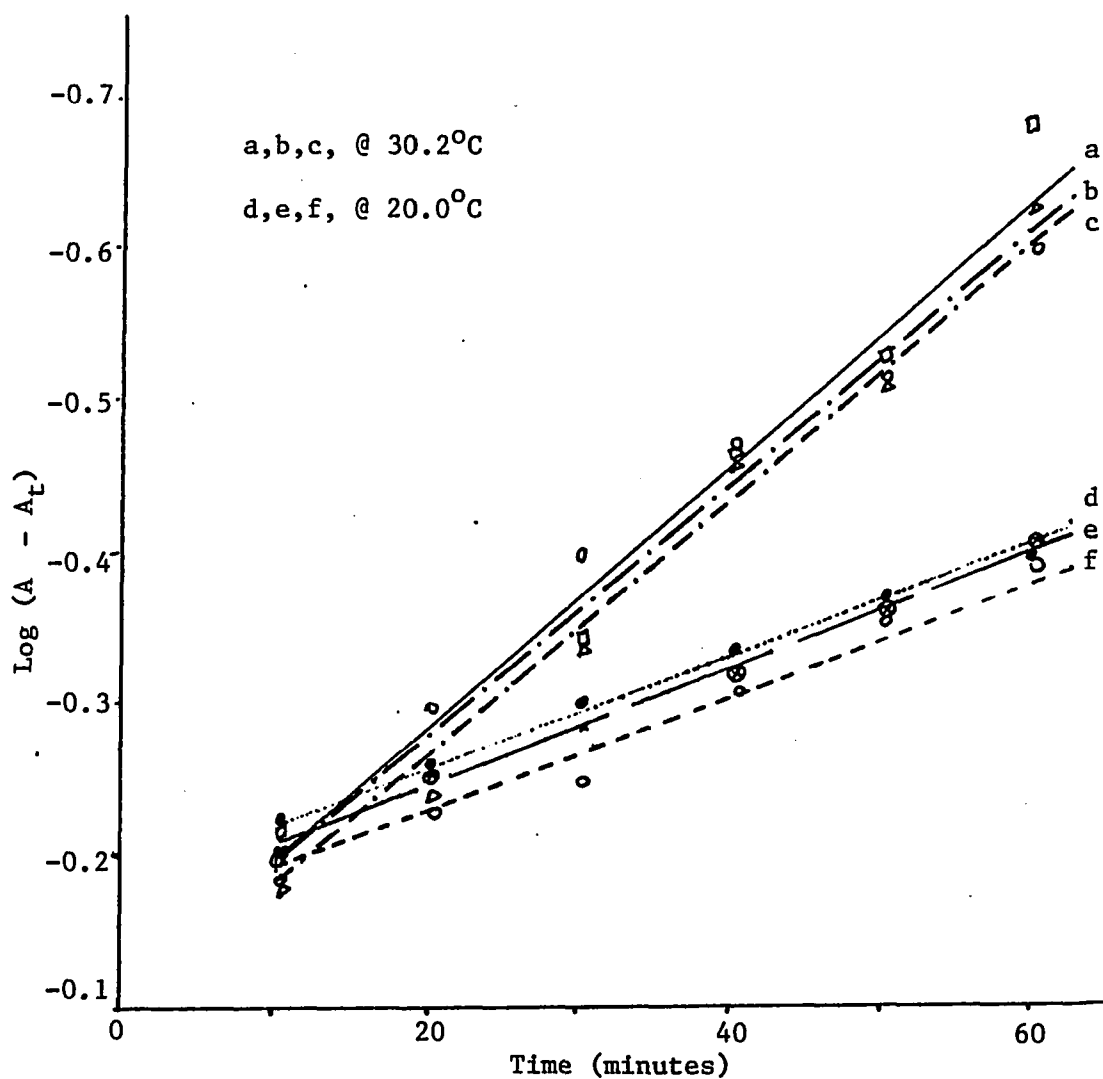


Figure 18. Kinetic Plots for pH 5.02 for Cr(II) - EDTA Reaction (numbers indicate trials).

Table 4

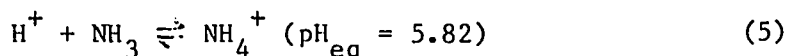
Rate Constants for the Reaction Between Chromium (III) Ion
and 0.1M Ethylenediaminetetraacetic Acid at Various Temperatures
and Hydrogen Ion Concentrations

Cr (III) Millimoles per liter	Temp °C	pH	Number of runs	K x 10 ³ sec ⁻¹	
5.8	22.00	5.02	3	0.97	0.06
5.8	22.00	5.50	3	1.14	0.05
5.8	30.22	5.02	3	2.01	0.07
5.8	30.22	5.50	3	2.16	0.10

added titrant.

Acid-Base Titrator

The application to photometric endpoint detection was demonstrated with various indicators in neutralization reactions with standard solutions of 0.040M NH_3 and 0.010M HCl . The hydrochloric acid solution was prepared from a one liter dilution of an Acculute standard volumetric solution prepared by Anachemia Chemicals LTD., Champlain, NY. The ammonia solution was prepared by diluting 7.6 mL of 30% concentrated ammonia to one liter. Then a one to ten dilution was made followed by standardization against the 0.010M HCl solution using bromocresol purple ($\text{pK} = 6.21$) as the indicator following the reaction in Equation 5 (39):



The bromocresol purple visual color change is purple to yellow, thus requiring absorbance measurements of yellow to yellow-green. This was not used out of concern that the resolution of the monochromator might not adequately resolve the wavelengths of interest. In an effort to test the system with various color combinations, bromothymol blue ($\text{pK}_a = 7.84$, blue to yellow) and phenol red ($\text{pK}_a = 7.13$, yellow to red) were used. The reactions were followed at the wavelength of maximum absorbance for each colored indicator species with the endpoint then being calculated for each wavelength. The endpoint was also calculated as a function of both wavelengths since as one indicator species disappears, the other forms. Thus, by following both wavelengths and determining when the maximum change

in absorbance occurs per volume change, the results should be an endpoint more accurate than the one obtained from following either wavelength independently. This method of endpoint determination is illustrated in Figure 19 for phenol red indicator in the neutralization reaction.

The results of an NH_3 vs. HCl titration using phenol red indicator and employing 430 and 620 nm as the wavelengths of interest are shown in Table 5. End points obtained using bromothymol blue indicator with 440 and 620 nm as the wavelengths of interest may be seen in Table 6. The experimentally determined end points obtained using the single wavelength method for phenol red indicator are higher than the calculated end point volume. This is also true for the bromothymol blue indicator although the values using the bromothymol blue series are slightly higher than those from the phenol red indicator series. The precision of the end points volumes is acceptable; when using the dual wavelength end point technique,

the end point still exhibits a slightly positive bias but the precision increases even when varying indicators. The unequal magnitudes of scattered light can cause shifts in the baseline at the different wavelengths. This can cause a greater uncertainty in the resulting endpoints which could account for the variance when using the single wavelength method for end point determination.

Complexometric Titrations

The EDTA titration of calcium using calcein indicator may be

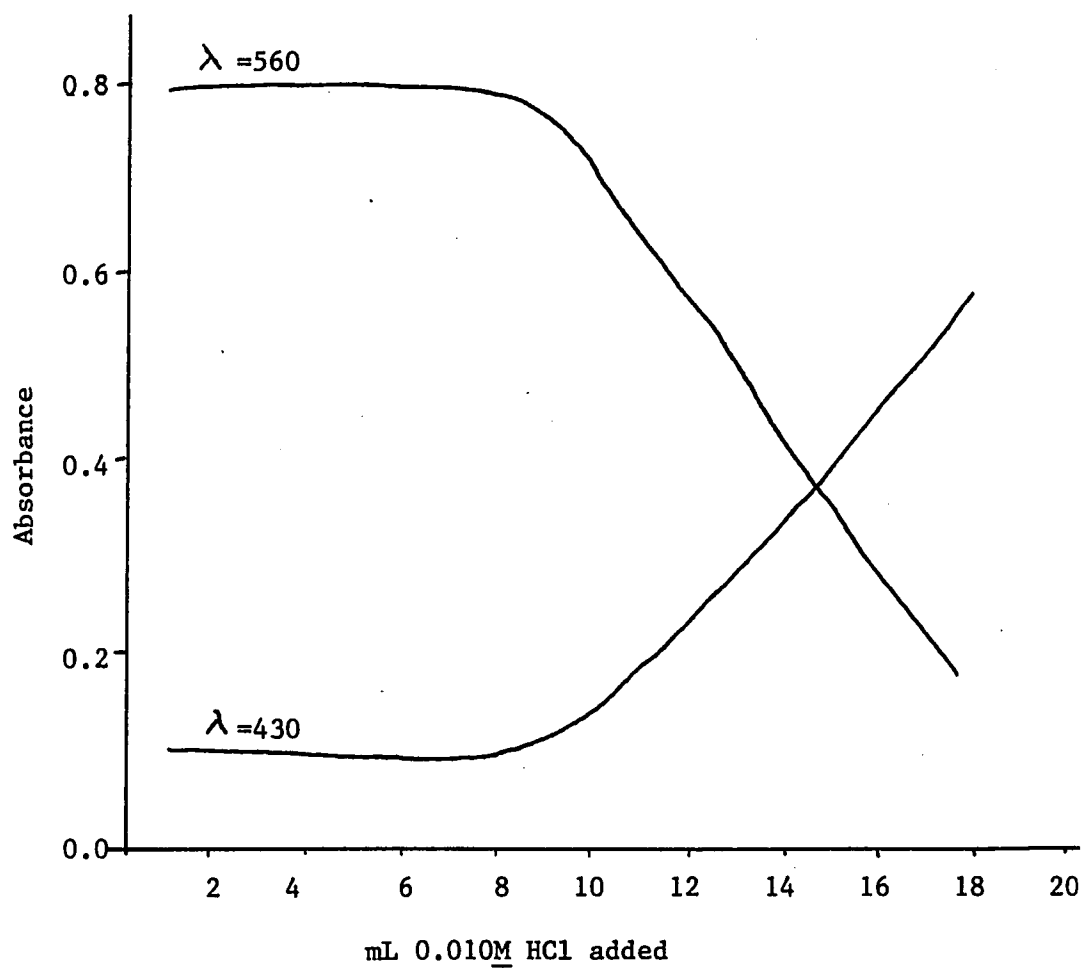


Figure 19. End Point Determination for 25mL 0.040M NH_3 vs. 0.010M HCl Using Phenol Red Indicator

Table 5

Determination of Neutralization Endpoints for 0.0100 M HCl in
25.00 mL 0.0400M NH_3 with Phenol Red Indicator (Expected
Endpoint Volume 10.04 mL)

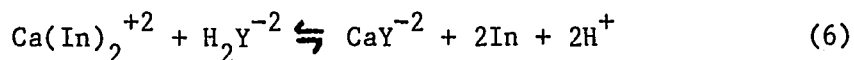
Sample No	Experimentally Determined Endpoint Volume of HCl					
	430 nm		560 nm		combined	
	vol	dev	vol	dev	vol	dev
1	10.07	0.03	10.09	0.05	10.08	0.04
2	10.12	0.08	10.27	0.23	10.10	0.06
3	10.23	0.19	10.19	0.15	10.13	0.09
4	10.20	0.16	10.15	0.11	10.06	0.02
5	10.28	0.24	10.23	0.17	10.10	0.06
	$\bar{v}=10.18$	$s=0.08$	$\bar{v}=10.19$	$s=0.07$	$\bar{v}=10.09$	$s=0.03$

Table 6

Determination of Neutralization Endpoints for 0.0100M HCl in
25.00 mL 0.0400M NH_3 with Bromthymol Blue Indicator (Expected
Endpoint Volume 10.04 mL)

Sample No	Experimentally Determined Endpoint Volume of HCl					
	440 nm		620 nm		Combined	
	vol	dev	vol	dev	vol	dev
1	10.10	0.06	10.08	0.04	10.12	0.08
2	10.24	0.20	10.19	0.15	10.17	0.13
3	10.06	0.02	10.10	0.06	10.08	0.04
4	10.32	0.28	10.21	0.17	10.09	0.05
5	10.18	0.14	10.32	0.28	10.14	0.10
	$\bar{v}=10.18$	$s=0.10$	$\bar{v}=10.17$	$s=0.12$	$\bar{v}=10.12$	$s=0.04$

used to illustrate end point detection for a photometric complexation titration. At the end point for the titration, the calcium-calcein complex is broken by reaction with excess EDTA causing the color to change from the fluorescent yellow-green to brown as shown in Equation 6:



An EDTA solution was prepared by dissolving 3.72 g EDTA in one liter of double distilled water. The 0.02% calcein indicator was prepared by dissolving 20.0 mg calcein in 100.0 mL doubly distilled water with 0.10M KOH to aid its dissolution. A 1.0% KCN solution was made by dissolving 1.0 g KCN in 100.0 mL doubly distilled water. A 5.0M KOH solution was prepared by dissolving 27.998 g KOH in 100.0 mL distilled water. The EDTA was then standardized against a stock solution of 0.012586M CaCO_3 solution as described by Diehl (40). The results of the colorimetric end points may be found in Table 7. The average experimental endpoint appears to be negatively biased relative to the titrations using visual endpoint detection. This may be the result of the photometric system being more sensitive to the color change than is the eye.

Fluorometer

Fluorescence intensity measurements also can be used in end point determinations using the fiber optic system. Since fluorescent radiation is emitted at all angles to the excitation radiation, the removal of the probe tip containing the mirror permits essentially only emitted light from the solution to enter the fiber optic probe.

Table 7

Endpoint Determination of 0.012414M EDTA vs. 10mL 0.012586M CaCO_3
 Using 0.02% Calcein Indicator (Visual Endpoint Volume: 10.14 mL)

Sample No	Experimentally Determined Endpoint Volume			
	photometric		Fluorescent	
	vol	dev	vol	dev
1	10.18	0.04	10.26	0.12
2	9.92	-0.22	10.24	0.10
3	10.23	0.09	10.20	0.06
4	9.82	-0.32	9.98	-0.16
5	9.88			
	$\bar{v}=10.01$	$s=0.19$	$\bar{v}=10.17$	$s=0.13$

Table 8

1,2-Dichlorofluorescein Endpoint Determination of 0.01000M HCl
 vs. 25 mL 0.0400M NH_3 (Expected Endpoint Volume: 10.04 mL)

Sample No	Experimentally Determined Endpoint Volume	
	vol	dev
1	9.78	-0.26
2	9.96	-0.08
3	9.88	-0.16
4	9.68	-0.36
5	9.72	-0.32
	$\bar{v}=9.80 \text{ mL}$	$s=0.12$

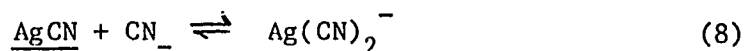
The light is then returned to the monochromator where the fluorescent peak is isolated by the photometer/computer system. The complexometric EDTA titration of calcium using calcein as indicator also exhibits fluorescence prior to the endpoint and is quenched at the endpoint. The data for this titration may also be seen in Table 7. The scatter of data observed for the fluorescence technique is not significantly different from that obtained using the colorimetric end point determination. The fluorescence endpoint detection appears to have a positive bias relative to the expected endpoint volume. The reason for this bias is not immediately obvious. Perhaps some background fluorescent species are present and becomes quenched only in excess of EDTA.

1,2-Dichlorofluorescein may be employed as an indicator for some neutralization reactions. Standard solutions of 0.040M NH_3 versus 0.010M HCl , were used to investigate the fluorescent acid-base end point characteristics. The same standard solutions used in the colorimetric endpoint determinations were employed. As shown in Table 8, the precision is poorer relative to photometric technique. Also there appears to be evidence of a negatively biased determination error. These results might have greater precision if filters to isolate the excitation wavelength were used on the incoming light in order to remove incident radiation of the same wavelength as the emitted radiation. This would result in less scattered light returning to the monochromator. The presence of a negatively biased determinate error is apparent and might be

explained due to the disparity between the equivalence point pH of 5.82 versus the pH range of the indicator of 4-6 for visual standardization measurements.

Nephelometry and Turbidimetry

Scattered radiation due to a particulate phase can be measured by either nephelometry or turbidimetry. These measurements have similar optical arrangements as fluorescence and absorption techniques except that they measure scattered radiation instead of absorbed radiation. Nephelometric measurements can readily be made with a procedure analogous to the fluorescence measurements, measuring the power of the beam scattered at right angles to the incident beam. A plot of the amount of light scattered versus concentration frequently produces a pseudo linear relationship analogous to the Beer's law curve in photometric analysis. The endpoint in precipitation reactions involving non-absorbing ions can be determined by monitoring the wavelength of greatest sensitivity. This was demonstrated using Ag^+ and CN^- as the non-absorbing ions and following the reactions in Equations 7 and 8:



The first end point involves the formation of the AgCN precipitate while the second endpoint depends on the dissolution of the precipitate in excess CN^- . An Acculute standard volumetric solution of 16.99 g AgNO_3 was diluted to one liter to give a 0.1001N solution. A solution was prepared by dissolving 0.65 g KCN in one liter of

doubly distilled water, was standardized by adding 3.0 mL NH_3 (concentrated) and 0.10 g KI to a 20.00 mL aliquot and then titrated with 0.1001N AgNO_3 standard until the first sign of permanent opalescence in solution. The data for this light scatter system can be found in Table 9. The second end point should be twice the first. In actuality it appears to be less than the expected value. The poor precision in the observed data may be due to a lack of reproducibility in particle size from one titration to another. Factors such as temperature, stray light, and the rate of reagent addition are all factors which can affect particle size but are difficult to precisely control during the course of a titration.

Turbidimetric endpoints of the same Ag^+ versus CN^- system are found in Table 10. As in the nephelometric measurements, the first end point is greater than expected and the second end point again less than twice the first. As before, the size of the particles could be an important variable contributing to the scatter of the data.

Emission Photometer

The system was also used to evaluate spectral emission measurements. The emission program and flow chart can be found in Appendix D. No quantitative emission analyses were carried out due to the fact that neither suitable electrical or flame excitation sources were readily available. Nevertheless emission spectra of both a tungsten filament and a sodium vapor source were obtained and may be seen in Figures 20 and 21, respectively. It would appear that the

Table 9

Nephelometric Endpoint Determination of 0.01001N AgNO_3 vs. 20 mL
0.004995 N KCN (Expected Endpoints: 9.98 mL, 19.96 mL)

Sample No	Experimentally Determined Endpoint		Volume of AgNO_3	
	1st Endpoint		2nd Endpoint	
	vol	dev	vol	dev
1	11.08	1.10	21.03	1.07
2	11.51	1.63	21.12	1.13
3	11.81	1.93	21.20	1.24
4	11.23	1.25	21.18	1.22
5	*		20.63	0.73
	$\bar{v}=11.41$	$s=0.32$	$\bar{v}=21.03$	$s=0.23$
* Rejected Using Q test criterion (39)				

Table 10

Turbidimetric Endpoint Determination of 0.1001N AgNO_3 vs. 20.00 mL
0.004995 N KCN (Expected Endpoints: 9.98 mL, 19.96 mL)

Sample No	Experimentally Determined Endpoint		Volume of 0.1001N AgNO_3	
	1st Endpoint		2nd Endpoint	
	vol	dev	vol	dev
1	11.31	1.33	21.41	1.45
2	11.24	1.26	21.27	1.31
3	11.03	1.05	20.98	0.02
4	11.20	1.22	21.14	1.18
5	11.14	1.16	21.08	1.02
	$\bar{v}=11.18$	$s=0.11$	$\bar{v}=21.18$	$s=0.17$

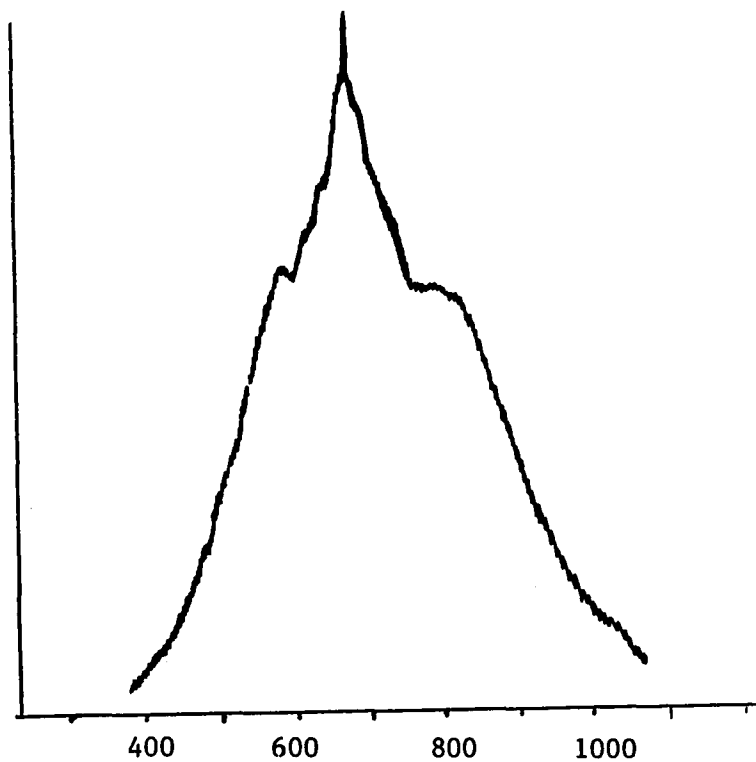


Figure 20. Emission Spectrum of Tungsten Source Showing an Uncorrected Detector Response.

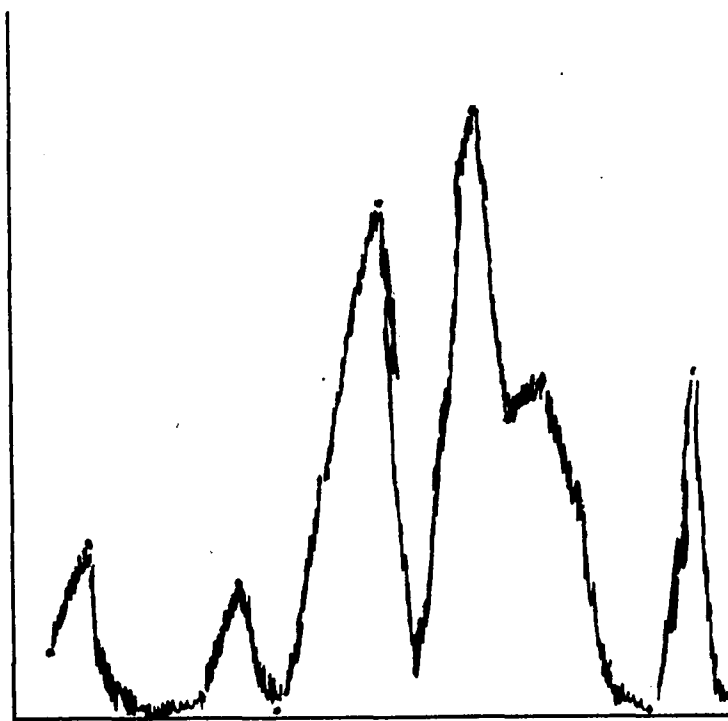


Figure 21. Emission Spectrum of Sodium Vapor Source Showing an Uncorrected Detector Response.

application of this instrument to quantitative emission measurements should be reasonably straight forward.

Conclusions

Microprocessor System

The data obtained from the microprocessor controlled rapid scanning fiber optics spectrophotometer show one of many possible applications of the system. Due to limited memory, transmittance calculations using the reflectance data were the only calculations performed although the capability for derivative and emission spectra is also available as well as output to a storage oscilloscope and subsequently to an x-y plotter for hard copy of the spectra.

Apple/Isaac System

The computer controlled rapid scanning fiber optics spectrophotometer is well suited for titrations. The ability to monitor several wavelengths simultaneously provides great flexibility in the titrations of mixtures and allows for multiple components to be analyzed. The rapid scan capability allows for multiple wavelength monitoring during kinetics reactions with the data being stored on disk for later calculations. The probe tip returns the modified emission spectra to the monochromator port allowing for transmittance, absorbance and turbidimetric spectral calculations. Removal of the probe tip permits the sample attenuated light to return to

the monochromator port providing reflectance, fluorescence and nephelometric data.

The experimental data show much promise. Improvements of the system could include a light probe with the capability to filter out certain wavelengths, increasing the sensitivity for endpoint detection. Another advantage would be to build a binary coded decimal (BCD) interface to control the wavelength marker position, thus making the system more automated. Custom software using Apple /BASIC could be designed for any specific application or data massaging with the user accessing the data files required.

APPENDIX A
Rofin Monochromator

Rofin Monochromator

The Rofin Model 6000 monochromator is the basis of a compact and highly versatile system for displaying and measuring optical spectra. The monochromator unit consists of an optical system and an electrical system within the same housing (36).

The optical system uses a blazed diffraction grating in a side by side Ebert configuration as illustrated in Figure 7. The grating is continuously rotated by a DC motor, producing a repeatedly swept optical spectrum at the output slit. A reflecting encoder disk attached to the motor shaft, an infrared-emitting diode and detector produce a trigger pulse for the display oscilloscope. The encoder disk serves a dual purpose, since it also generates a train of pulses that are used by the Wavelength Marker accessory (described below) to generate an accurate wavelength calibration scale. Four optical bandwidths are available with a specially designed slit plate; 2, 5, 10 and 20 nm.

The electrical system is comprised of a DC motor and associated drive circuitry, an oscilloscope trigger pulse generator, internal voltage stabilizing circuitry, and a high gain trans-impedance amplifier for use with the Rofin detector assembly. An accessory socket for the wavelength marker is also provided as

part of the electrical system.

The wavelength marker unit increases the wavelength accuracy from 8 nm to 0.5 nm. The wavelength marker unit combines a number of features to increase the accuracy and versatility of the monochromator system. They are as follows:

1. Scan period Control - The scan period can be synchronized with a choice of three signals (a) a multiple of the mains supply frequency, (b) an internal adjustable oscillator, or (c) an external signal source.
2. Phase Control - In relation to (a) above this allows examination of the mains driven optical sources at different regions on the mains cycle.
3. Wavelength Marker Selector - A four digit thumbwheel switchbank generates a pulse on channel 2 of the oscilloscope display. The marker pulse can be moved in the wavelength domain and used to locate points of interest in the spectrum.
4. Trigger Delay Control - This feature adjusts the width of the trigger pulse in the scope. With this it is possible to move the trigger to a region of interest and then expand the wavelength scale by changing the oscilloscope time base control. The expanded display will still contain the selected wavelength marker and other wavelength pulses on either side of the marker, thereby making it possible to obtain very accurate wavelength measurements.

APPENDIX B
Heath Hardware

Heath Hardware

The Motorola 6800 central processing unit (CPU), Figure 1B, requires a single five volt power supply and two precisely defined overlapping clock signals, labeled as 01 and 02. The 01 clock signal is used for internal instruction sequencing, while the 02 clock signal is used as an I/O control line for timing and sequencing the 6800 with I/O devices. The sixteen address lines, A0 through A15, and eight bidirectional data lines, D0 through D7, make up the external address and data busses.

Control operations for read/write operations are provided by the valid memory address (VMA) and the read/write line (R/W) control lines. The R/W line indicates the direction of data transfer, which is at a logic 1 for "read" and at a logic 0 for "write". The VMA line goes to a logic 1 whenever the CPU places a valid 16-bit memory address on the address bus.

Hardware interrupts are provided through the reset (RESET), interrupt request (IRQ), and non-maskable interrupt (NMI) pins on the 6800 chip. These are all vectored interrupts that directly access interrupt service routines at specific memory locations. RESET is used for system initialization and restart. The IRQ input is a maskable interrupt line that is ignored if the interrupt (I) flag in the internal condition code register is set. The

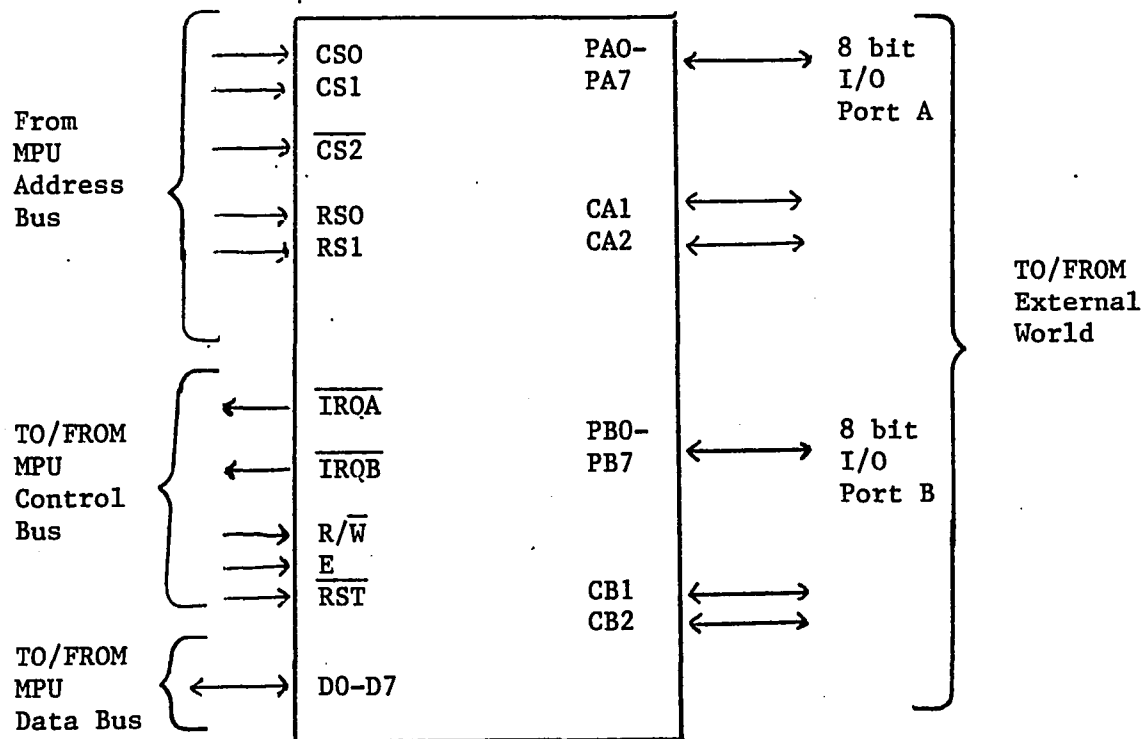


Figure 1B. Block Diagram of MC 6821 Peripheral Interface Adapter

NMI input, however, can never be masked out and is normally used for emergency interrupt situations. The CPU automatically stores the contents of its internal registers in a stack in read/write memory when either the IRQ or the NMI interrupts are acknowledged.

External bus control is provided with the bus control lines, bus available (BA), data bus enable (DBE), and three state control (TSC). These lines are used to effectively disconnect the CPU from the external bus system in order to allow direct memory access (DMA) by external devices.

A large portion of I/O processing is handled by intelligent peripheral chips such as the Motorola 6821 peripheral interface adapter (PIA) with the data being transferred along the microprocessor's bidirectional data bus. The PIA is organized as two sets of data direction registers (DDRA and DDRB), control registers (CRA and CRB), and data buffers (DBA and DBB) with their associated control lines CA1, CA2, CB1, and CB2 as shown in Figure 2B. The data direction registers define the direction of data transfer, input or output. The control registers are used to set up the data direction registers and define responses for the corresponding data buffers and control lines. Since there are only two register select lines (RS0 and RS1) to select these locations, a bit in each of the two control registers is used in conjunction with RS0 and RS1 to specify the registers or data buffers.

The chip select (CS0, CS1, and CS2) and register select

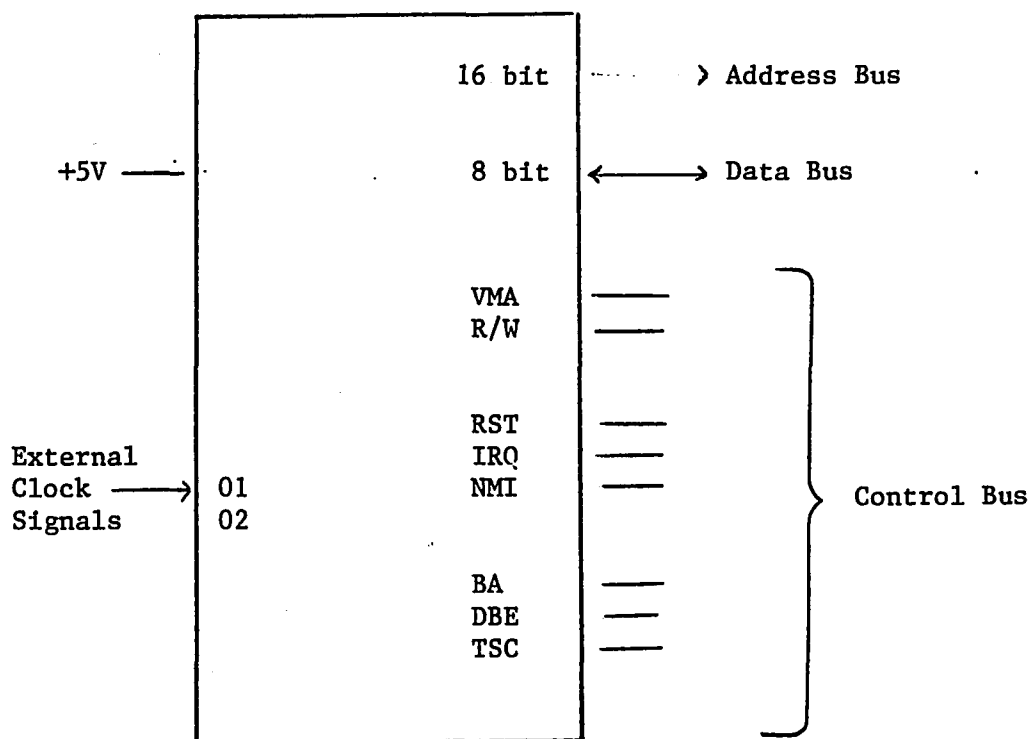


Figure 2B. Block Diagram of the Motorola 6800 Central Processing Unit.

inputs are obtained from the microprocessor address lines with direction determined by the R/W line, high level indicating "read" and low indicating "write" to the PIA. An enable (E) input to the PIA is used for conditioning interrupt control and timing peripheral control signals synchronizing all logic and timing within the PIA. The "A" and "B" I/O ports (PA0 through PA7 and PB0 through PB7) provide the connections for the data buffers to external devices.

The four control lines can be programmed as interrupts between the external device and the PIA, providing handshaking to set up and acknowledge the exchange of data. There are two interrupt request lines (IRQA and IRQB) which specify the conditions under which an interrupt can occur for either I/O port.

Communications between the CPU and the 6821 occur on the bidirectional data bus, D0 - D7. All the registers are cleared, set to zero when the input to the reset is low.

APPENDIX C
Microprocessor Software and Flowcharts

Microprocessor Software

Set-up Subroutine

86	04	LDA	Set PIA side A as input
B7	8001	STA	
B6	8000	LDA	Check for low wavelength reading
84	80	ANDA	
81	80	CMPA	
26	05	BNE	
7F	0006	CLR	Clear wavelength reading counter
20	F2	BRA	Go back to taking wavelength reading
7C	0006	INC	Increment wavelength reading counter
86	32	LDA	See if 50 "0" readings have been taken
91	06	CMPA	
23	E9	BLS	
7F	0006	CLR	Clear wavelength counter
86	8000	LDA	Check for high cycle
84	80	ANDA	
81	80	CMPA	
26	F7	BNE	
7C	0006	INC	Increment wavelength counter
96	07	LDA	Compare counter with desired wavelength
91	06	CMPA	If not equal, go back to checking for high
26	EE	BNE	

Make sure data is taken on wavelength pulse

86	04	LDA	Set PIA side A as input
B7	8001	STA	
B6	8000	LDA	
84	80	ANDA	Check for low cycle of wavelength pulse
81	00	CMPA	
26	F7	BNE	
B6	8000	LDA	
84	80	ANDA	Check for high cycle of wavelength pulse
81	80	CMPA	
26	F7	BNE	
86	00	LDA	Set PIA side B as output
B7	8001	STA	
B7	8000	STA	
86	40	LDA	Pulse A/D converter
B7	8000	STA	
86	04	LDA	
B7	8001	STA	Set PIA side A as input
B6	8000	LDA	
84	20	ANDA	Wait for EOC pulse from A/D converter
81	20	CMPA	
27	F7	BEQ	
3F		SWI	Go to software interrupt routine

FE	0002	LDX	Check to see if all data taken, going
BC	0004	CPX	back to wavelength pulse routine if not
26	C8	BNE	done
39		RTS	Go back to monitor routine

Interrupt Subroutine

86	04	LDA	Set PIA side A for input of data
B7	8001	STA	
B7	8003	STA	
FE	0002	LDX	Load index register with pointer
B6	8000	LDA	Load MSB and store in memory
A7	00	STA X	
08		INX	Increment pointer
B6	8002	LDA	Load LSB and store in memory
A7	00	STA A	
08		INX	Increment pointer
FF	0002	STX	Store pointer
3B		RTI	Return from interrupt routine

%T Calculation Subroutine

86	60	LDA	Load number of data points into memory 0005
97	05	STA	
86	0C	LDA	Load number of bits into memory 0004
97	04	STA	
FE	0006	LDX	Load index register with data point
A6	00	LDA X	Put baseline MSB in 000A
97	0A	STA	
08		INX	
A6	00	LDA X	Put baseline LSB in 000B
97	0B	STA	
08		INX	
FF	0006	STX	Put next data point into memory 0006
FE	0002	LDX	
A6	00	LDA X	Sample MSB in A
08		INX	
E6	00	LDB X	Sample LSB in B
08		INX	
FF	0002	STX	
7F	000C	CLR	Quotient Clearing LSB
7F	000D	CLR	Quotient Clearing MSB
78	000C	ASL	
79	000D	ROL	
91	0A	CMPA	A-0A (MSB)
2D	09	BLT	
D0	0B	SUBB	B-0B into accumulator B (LSB)
92	0A	SBCA	A-0A-C into accumulator A (MSB)
25	03	BCS	Check to see if negative

7C	000C	INC	Increment quotient
58		ASLB	Shift
49		ROLA	
7A	0004	DEC	Decrement number of bits left to subtract
7D	0004	TST	See if done
26	E3	BLS	Continue process if not done
BD	0F60	JSR	Jump to storage subroutine
BD	0F08	JSR	Jump to BCD conversion subroutine
7A	0005	DEC	Decrement number of data points
7D	0005	TST	See if done
27	02	BEQ	Continue if not done
20	AD	BRA	
39		RTS	Go back to monitor routine

BCD Conversion and Storage Subroutine

CE	0F38	LDX	Clear temporary data storage locations
4F		CLRA	
A7	00	STA X	
08		INX	
8C	0F3F	CPX	
26	F8	BNE	
CE	0F32	LDX	Load hex value
96	0C	LDA	Load transmittance LSB
D6	0D	LDB	Load transmittance MSB
A0	00	SUBA	Transmittance - hex value
E2	01	SBCB	
25	08	BCS	
6C	06	INC	Increment counter
97	0C	STA	Put new values in registers and do again
D7	0D	STB	
20	F2	BRA	
08		INX	Increment index register for next conversion
08		INX	
8C	0F38	CPX	See if done
27	0F	BEQ	
20	E5	BRA	Go to packing and storage portion of subroutine
9A			019A = 0.1
01			
29			0029 = 0.01
00			
04			0004 = 0.001
00			
00			
			Data locations
00			
FE	0008	LDX	Load index register with storage location

B6	0F36	LDA	Load A with MSB
A7	00	STA X	
08		INX	
B6	0F3A	LDA	
48		ASLA	Shifting decimal values (packing)
48		ASLA	
48		ASLA	
48		ASLA	
BB	0F3C	ADDA	Add LSB to MSB
A7	00	STA X	Put packed value into index register
08		INX	Increment index pointer
FF	0008	STX	Store index pointer
39		RTS	Go back to monitor routine

Tiny Basic Reflectance Program

```
10 PR "THIS PRGRAM SET TAKES REFLECTANCE DATA, CALCULATES %T"
15 PR "IN BCD EQUIVALENTS AND OUTPUTS THE SPECTRUM TO THE
   O-SCOPE"
20 PR "THE SCAN STARTS AT 415 FOR CHROMATICITY CALCULATIONS"
30 B=USR(7188,4,2560)
35 PR "INPUT 1 WHEN YOU ARE READY TO TAKE BASELINE DATA"
40 INPUT X
50 C=USR(7188,4,2620)
55 C=USR(3584)
60 PR
65 PR "INPUT SAMPLE NUMBER WHEN YOU ARE READY TO TAKE SAMPLE
   DATA"
70 INPUT X
75 D=USR(7188,2,2680)
80 D=USR(7188,4,2620)
90 D=USR(3584)
95 PR
100 PR "TO OBTAIN %T VALUES IN BCD, ENTER 0"
105 PR "TO SEE REFLECTANCE SPECTRA ON THE O-SCOPE, ENTER 1"
110 PR "TO OBTAIN BOTH, ENTER 2"
120 INPUT Y
125 IF Y=1 THEN GOTO 175
130 A=USR(3744)
140 PR
150 IF Y=1 THEN GOTO 200
175 A=USR(3840)
180 PR "BCD VALUES HAVE BEEN CALCULATED AND ARE STORED BETWEEN"
185 PR "AB5 AND AF0 (HEX), GO BACK TO MON TO EXAMINE"
190 IF Y=0 THEN GOTO 220
200 A=USR(3904)
205 PR
210 PR "THE REFLECTANCE SPECTRUM OF SAMPLE ",X," IS ON THE
   O-SCOPE"
220 PR "INPUT SAMPLE NUMBER TO TAKE MORE DATA, IF YOU WISH"
230 PR "TO STOP ENTER 0"
235 INPUT X
240 IF X=0 THEN GOTO 75
250 END
```

Program for Chromaticity Coordinate Calculation

```

10  DISP "THIS PROGRAM WILL CALCULATE CHROMATICITY COORDINATES
    FOR REFLECTANCE STUDIES"
20  PRINT
30  DISP "INPUT THE REFLECTANCE VALUE FOR THE WAVELENGTH 415"
40  INPUT A
50  X=A*1.97
60  Y=A*.06
70  Z=A*9.6
80  DISP "INPUT THE REFLECTANCE VALUE FOR THE WAVELENGTH 445"
90  INPUT A
100 X=X+A*12.19
110 Y=Y+A*1.03
120 Z=Z+A*63.6
130 DISP "INPUT THE REFLECTANCE VALUE FOR THE WAVELENGTH 475"
140 INPUT A
150 X=X+A*5
160 Y=Y+A*3.94
170 Z=Z+A*37.36
180 DISP "INPUT THE REFLECTANCE VALUE FOR THE WAVELENGTH 505"
190 INPUT A
200 X=X+A*.07
210 Y=Y+A*12.29
220 Z=Z+A*6.56
230 DISP "INPUT THE REFLECTANCE VALUE FOR THE WAVELENGTH 535"
240 INPUT A
250 X=X+A*6.4
260 Y=Y+A*25.79
270 Z=Z+A*.86
280 DISP "INPUT THE REFLECTANCE VALUE FOR THE WAVELENGTH 565"
290 INPUT A
300 X=X+A*20.04
310 Y=Y+A*28.74
320 Z=Z+A*.08
330 DISP "INPUT THE REFLECTANCE VALUE FOR THE WAVELENGTH 595"
340 INPUT A
350 X=X+A*27.35
360 Y=Y+A*17.87
370 Z=Z+A*.03
380 DISP "INPUT THE REFLECTANCE VALUE FOR THE WAVELENGTH 625"
390 INPUT A
400 X=X+A*18.78
410 Y=Y+A*7.97
420 DISP "INPUT THE REFLECTANCE VALUE FOR THE WAVELENGTH 655"
430 INPUT A
440 X=X+A*5.47
450 Y=Y+A*2.03
460 DISP "INPUT THE REFLECTANCE VALUE FOR THE WAVELENGTH 685"

```

```
470 INPUT A
480 X=X+A*.77
490 Y=Y+A*.28
500 W=X+Y+Z
510 X=X/W
520 Y=Y/W
530 Z=Z/W
532 DISP
534 DISP
536 DISP
538 DISP
540 DISP "THE CHROMATICITY COORDINATES FOR THESE READINGS ARE:"
550 DISP "X= ",X
560 DISP "Y= ",Y
570 DISP "Z= ",Z
572 DISP
574 DISP
576 DISP
578 DISP
580 END
```

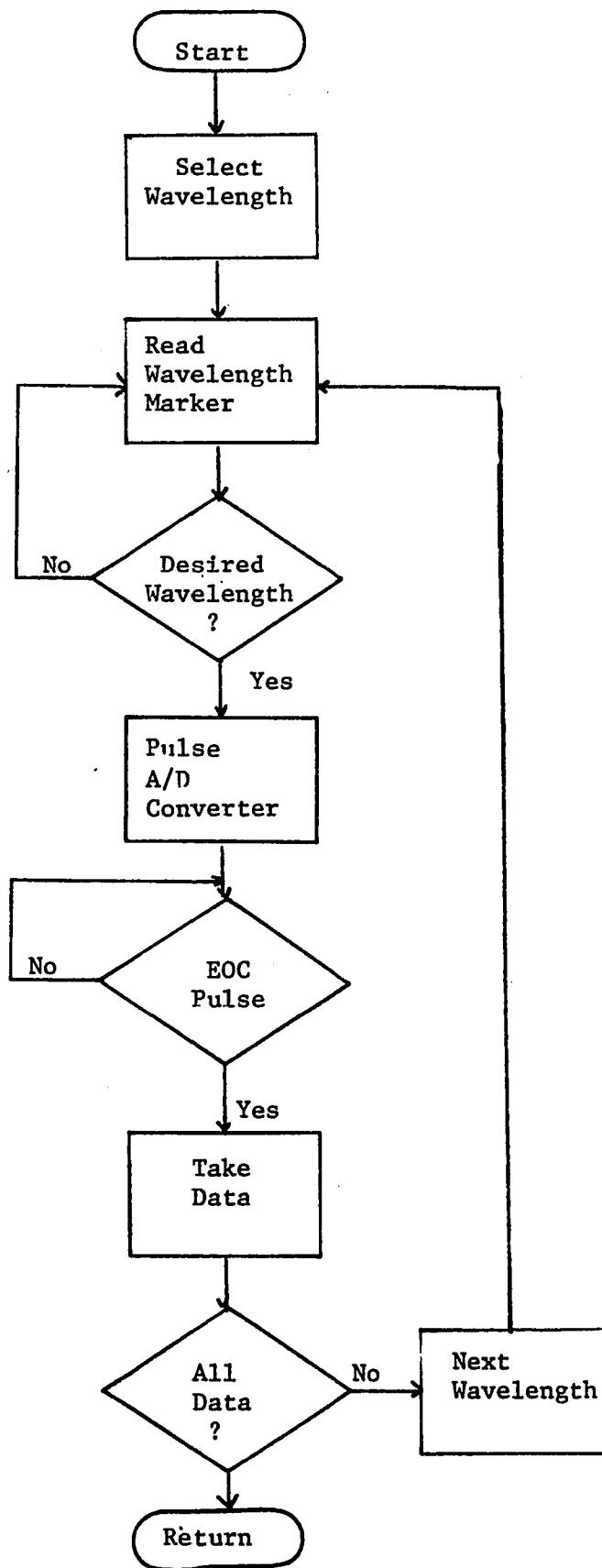


Figure 1C. Flowchart for Microprocessor Set-up Routine Used for Reflectance Data.

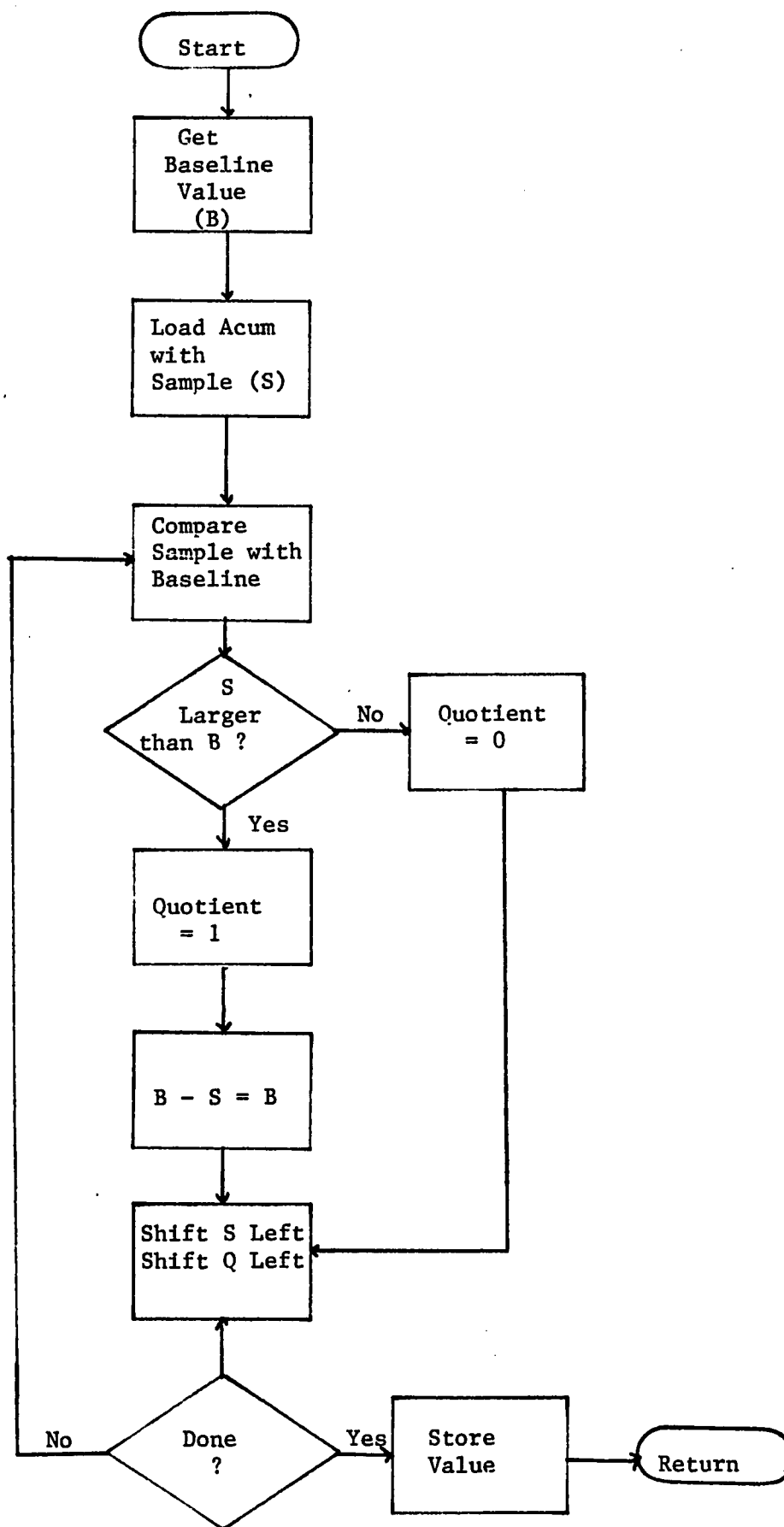


Figure 2C. Flowchart for Microprocessor Transmittance Calculation Subroutine.

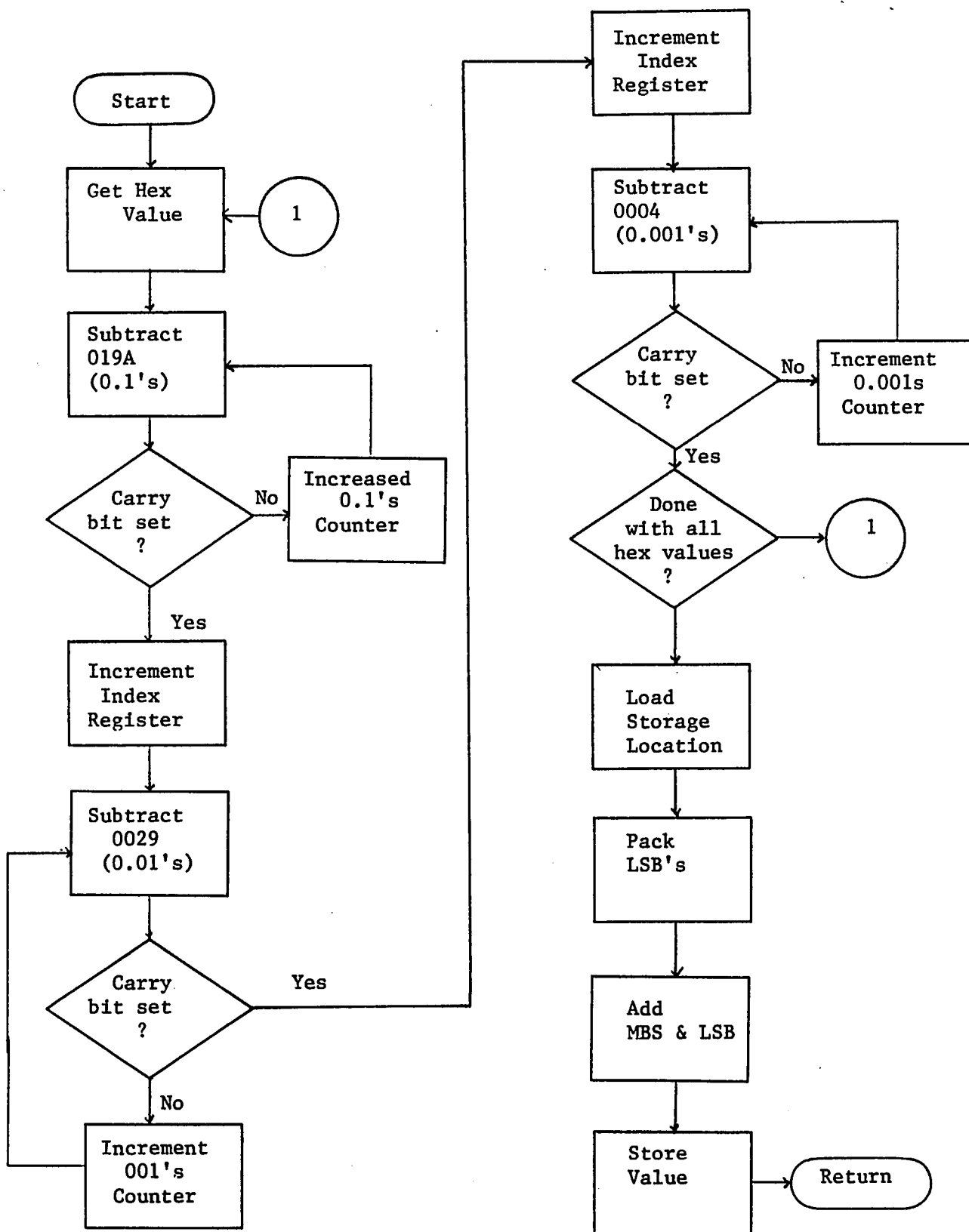


Figure 3C. Flowchart for Conversion of Hexidecimal Values to Binary Coded Decimal Values.

APPENDIX D

Software and Flowcharts for the Apple/Isaac System


```

LOAD EMISSION
]LIST
300 D$ = CHR$ (4)
310 :
330 X = PEEK. (116) * 256 + PEEK (115)
340 :
360 ADR = X - 690
370 :
390 PRINT D$: "BLOAD TRANSIENT.OBJ,A":ADR
400 :
410 J = 0
430 HIMEN: ADR
440 :
460 DIM AB%(160)
491 CALL ADR.AB%,0,0,1
492 DIM AC%(160)
494 CALL ADR.AC%,0,0,1
496 DIM AD%(160)
498 CALL ADR.AD%,0,0,1
500 DIM AE%(160)
501 CALL ADR.AE%,0,0,1
503 DIM AF%(160)
504 CALL ADR.AF%,0,0,1
506 DIM AG%(160)
508 CALL ADR.AG%,0,0,1
510 DIM AH%(160)
512 CALL ADR.AH%,0,0,1
514 DIM AI%(160)
516 CALL ADR.AI%,0,0,1
518 DIM AJ%(160)
520 CALL ADR.AJ%,0,0,1
522 DIM AK%(160)
524 CALL ADR.AK%,0,0,1
525 DIM AV(160)
526 DIM STD(160)
528 FOR N = 0 TO 160
540 AV(N) = (AB%(N) + AC%(N) + AD%(N) + AE%(N) + AF%(N) + AG%(N)
+ AH%(N) + AI%(N) + AJ%(N) + AK%(N)) / 10
545 VAR = (AB%(N) ^ 2 + AC%(N) ^ 2 + AD%(N) ^ 2 + AE%(N) ^ 2 +
AF%(N) ^ 2 + AG%(N) ^ 2 + AH%(N) ^ 2 + AI%(N) ^ 2 + AJ%(N) ^
2 + AK%(N) ^ 2 - 10 * AV(N) ^ 2) / 9
548 IF VAR < 0 THEN VAR = 0
550 STD(N) = SQR(VAR)
555 IF J < AV(N) THEN LET J = AV(N)
560 NEXT N
565 HOME : CALL 62450
570 & HIRES1
575 & SCROLLSET
576 & OUTLINE
580 & PLTFMT = 3
581 J = J / 100

```

```
585   FOR N = 0 TO 160
590   & NXTPLT = AV(N) / J
595   NEXT N
600   & PAUSE = 60
610   NEXT : HOME
620   INPUT "DO YOU WANT PRINT OUT OF DATA?  ":A$
630   IF A$ = "Y" THEN GOTO 700
640   INPUT "KEY IN NAME OF EMISSION SOURCE  ":N$
650   INPUT "KEY IN STARTING WAVELENGTH  ":A
660   PR# 1
670   PRINT N$,A
675   PRINT "",
680   PRINT "AVE","STD"
690   FOR N = 1 TO 50
691   PRINT AV(N),STD(N)
692   NEXT N
695   PR# 0
700   PRINT "EMISSION STUDY COMPLETED"
710   END
```

```
]LOAD FIBER OPTICS
]LIST
```

```
300 D$ = CHR$ (4)
310 :
330 X = PEEK (116) * 256 + PEEK (115)
340 : ONERR GOTO 2000
360 ADR = X - 690
370 : PRINT ADR
390 PRINT D$;"BLOAD TRANSIENT.OBJ,A";ADR
400 :
430 HIMEN: ADR
440 DIM MEAN(60)
442 DIM AV(60)
444 DIM AB(60)
446 DIM TRN(60)
450 DIM AD%(60)
455 HOME
460 PRINT " *MENU*";CHR$ (10)
470 PRINT "A. TAKE DATA"
480 PRINT "B. PRINT OUT DATA"
490 PRINT "C. GRAPH DATA"
500 PRINT "D. STORE DATA ON DISK"
510 PRINT "E. LOAD DATA FROM DISK"
515 PRINT "F. DERIVATIZATION OF CURRENT DATA"
517 PRINT "G. END"
520 PRINT : INPUT "SELECT ONE: ";A$
530 IF A$ = "" THEN & BEEP: GOTO 455
540 J = ASC (A$) - 64
550 IF J < 7 OR J > 0 THEN GOTO 455
555 HOME
560 ON J GOSUB 600,810,1500,1190,1000,1400,580
570 GOTO 455
580 END
600 INPUT "DO YOU WANT TO TAKE BASELINE DATA? ";A$
602 IF A$ = "N" THEN GOTO 690
603 HOME
604 INPUT "ARE YOU READY TO TAKE DATA? ";A$
605 & ARRAYCLR,AV
606 IF A$ = "N" THEN GOTO 603
608 FOR J = 0 TO 9
610 CALL ADR,AD%,0,0,1
620 FOR I = 0 TO 59
630 AV(I) = AD%(I) + AV(I)
640 NEXT I
650 & ARRAYCLR,AD%
660 NEXT J
```

```

690 HOME
700 INPUT "ARE YOU READY TO TAKE SAMPLE DATA? ";A$
710 IF A$ = "N" THEN GOTO 690
720 FOR J = 0 TO 9
730 & ARRAYCLR,AD%
740 CALL ADR,AD%,0,0,1
750 FOR I = 0 TO 59
760 MEAN(I) = AD%(I) + MEAN (I)
770 NEXT I
780 NEXT J
782 FOR I = 0 TO 59
783 IF AV(I) < 10 THEN GOTO 788
784 TRN(I) = (MEAN(I) / AV(I))
785 IF TRN(I) = 0 THEN GOTO 788
786 AB(I) = LOG(I) / TRN(I) / 2.303
788 NEXT I
804 RETURN
810 HOME
822 INPUT "ENTER SAMPLE NAME? ";N$: INPUT "ENTER SAMPLE NUMBER
";Z
824 PR# 1
825 PRINT CHR$(12)
826 PRINT N$,Z: PRINT " ": PRINT "%T", "ABS"
830 FOR I = 1 TO 49
840 PRINT TRN(I),AB(I)
850 NEXT I
855 PR# 0
880 RETURN
1000 INPUT "DO YOU WANT TO INPUT BASELINE DATA ?";Z$
1001 IF Z$ = "N" THEN GOTO 1091
1004 INPUT "NAME OF BASELINE FILE ";Z$
1005 PRINT D$;"VERIFY";Z$
1010 PRINT D$"OPEN ";Z$
1020 PRINT D$"READ ";Z$
1060 FOR I = 0 TO 59
1070 INPUT A:AV(I) = A
1080 NEXT I
1090 PRINT D$"CLOSE ";Z$
1091 INPUT "NAME OF SAMPLE FILE ";Z$
1092 PRINT D$"VERIFY ";Z$
1093 PRINT D$"OPEN ";Z$
1095 PRINT D$"READ ";Z$
1100 FOR I = 0 TO 59
1110 INPUT A:MEAN(I) = A
1120 NEXT I
1130 PRINT D$"CLOSE ";Z$: GOTO 782
1190 HOME
1202 PRINT "PRESS RTN WHEN DATA DISK IS INSERTED"
1204 GET A$
1205 INPUT "BASELINE OR SAMPLE ? ";A$
1206 INPUT "NAME OF TEXT FILE? ";Z$

```

```

1210 PRINT D$"OPEN ";Z$
1220 PRINT D$"DELETE ";Z$
1230 PRINT D$"OPEN ";Z$
1250 PRINT D$"WRITE ";Z$
1270 IF A$ = SAMPLE THEN GOTO 1320
1280 IF A$ ~ " " "BASELINE" THEN GOTO 1260
1290 FOR I = 0 TO 59
1300 PRINT AV(I)
1310 NEXT I
1316 PRINT D$"CLOSE ";Z$: RETURN
1320 FOR I = 0 TO 59
1330 PRINT MEAN(I)
1340 NEXT I
1350 PRINT D$"CLOSE ";Z$
1363 RETURN
1400 HOME
1405 IF A$ = "ABS" GOTO 1450
1410 FOR I= 1 TO 58
1415 TRN(I) = TRN(I) - TRN(I + 1)
1455 AB(I) = AB(I) - AB(I - 1)
1460 NEXT I
1480 RETURN
1500 HOME : INPUT "%T OR ABSORBANCE VALUES ";A$: CALL 62450
1501 INPUT "TITLE OF GRAPH? ";N$: CALL 62450: & LABEL = N$ AT 10,5
1505 & OUTLINE
1510 & HIRES2
1520 & SCROLLSET
1530 & PLTFMT = 2
1535 IF A$ = "ABS" GOTO 1600
1540 FOR N = 1 TO 59
1550 * NXTPLT = TRN(N) * 100
1560 & NXTPLT = TRN(N) * 100
1570 NEXT N
1590 GET A$: TEXT : RETURN
1600 FOR N = 1 TO 59
1605 IF AB(N) ~ 0 THEN LET AB(N) = 0
1610 & NXTPLT = AB(N) * 80
1615 & NXTPLT = AB(N) * 80
1620 NEXT N
1625 GET A$: TEXT : RETURN
2000 TEXT : HOME
2010 PRINT PEEK (222)
2015 POKE 216,0
2020 & PAUSE = 10
2030 GOTO 455

```

]PR#0

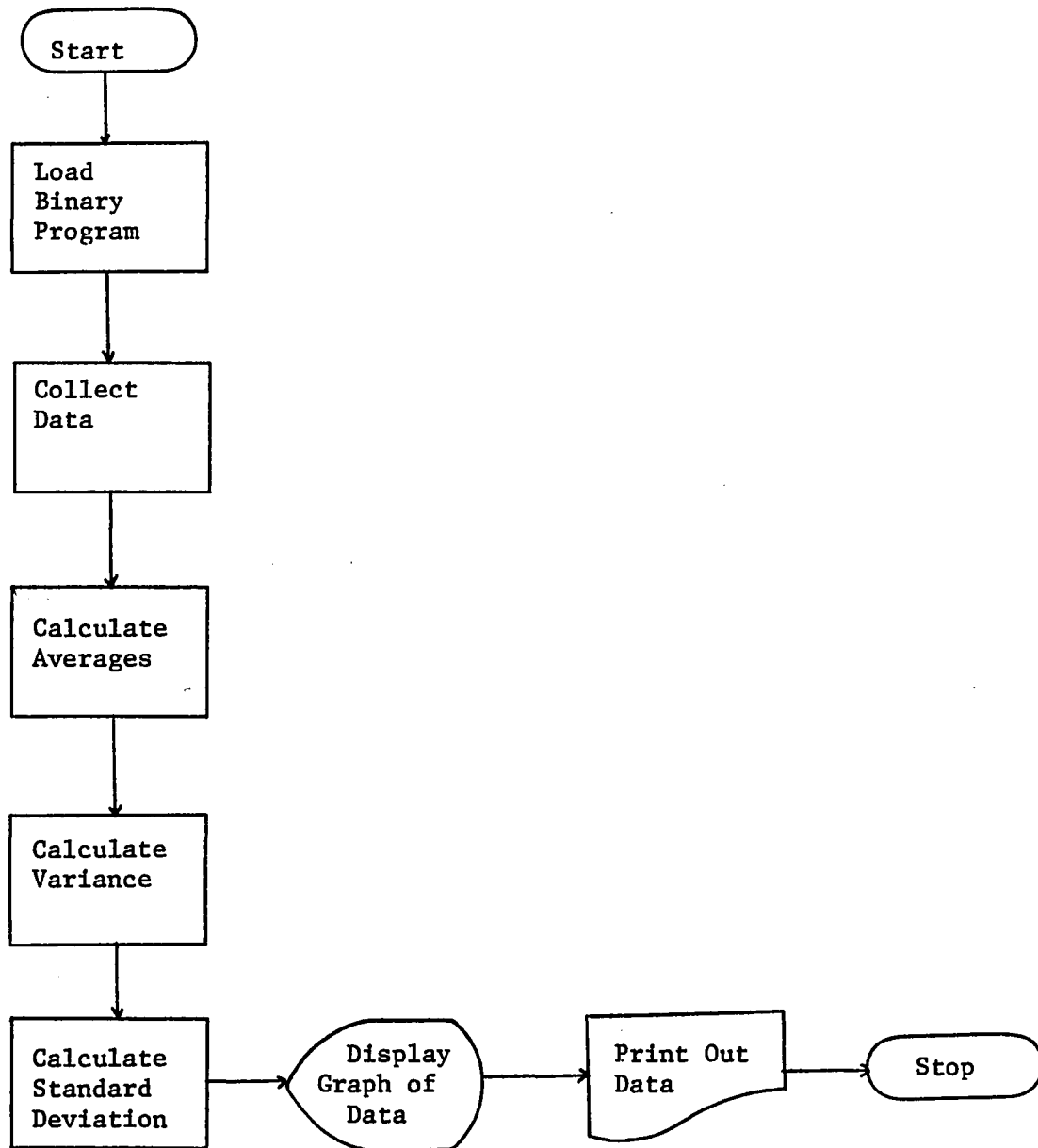


Figure 1D. Flow Chart for Emission Program

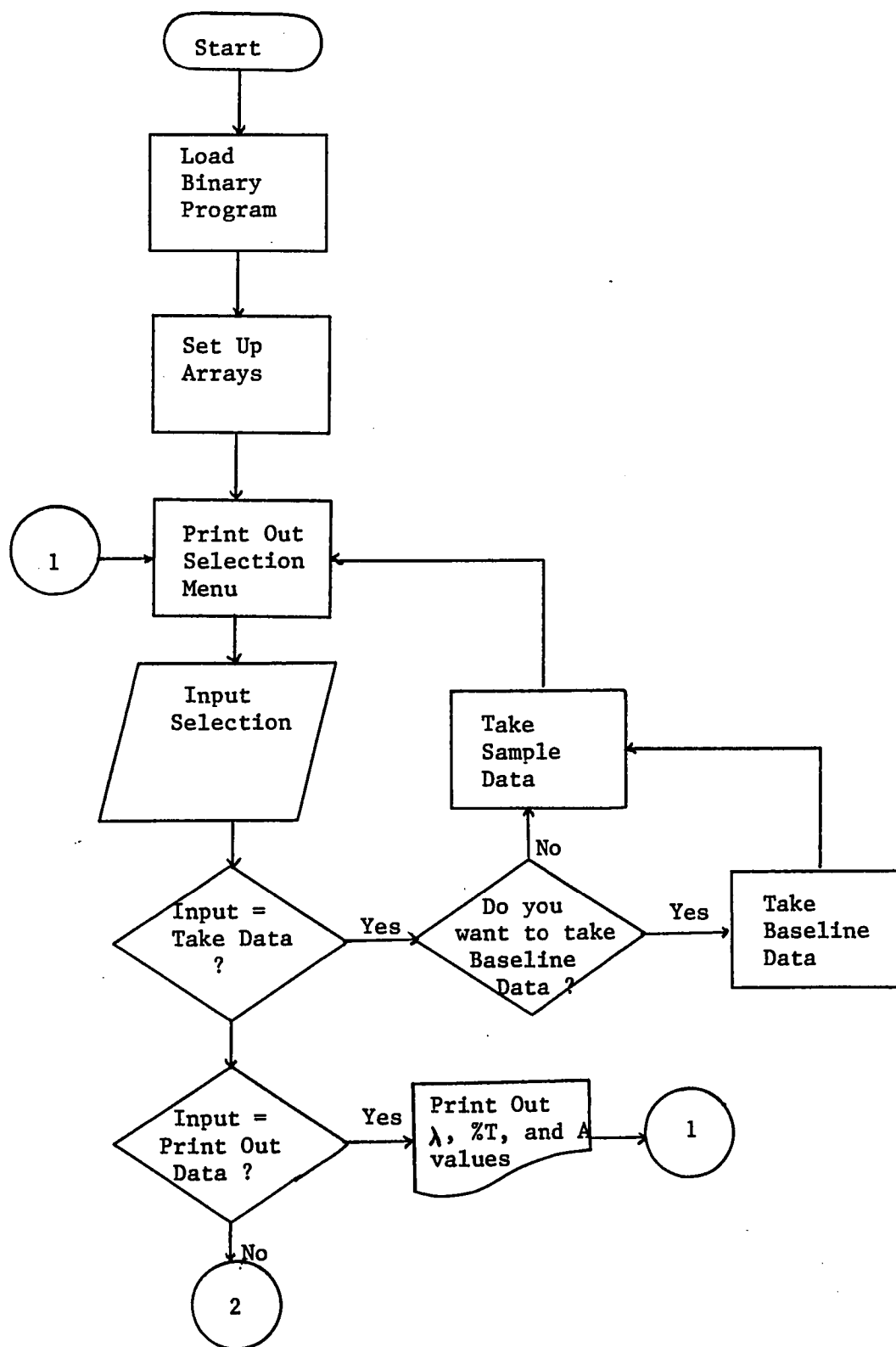


Figure 2D. Flow Chart for Fiber Optics Program.

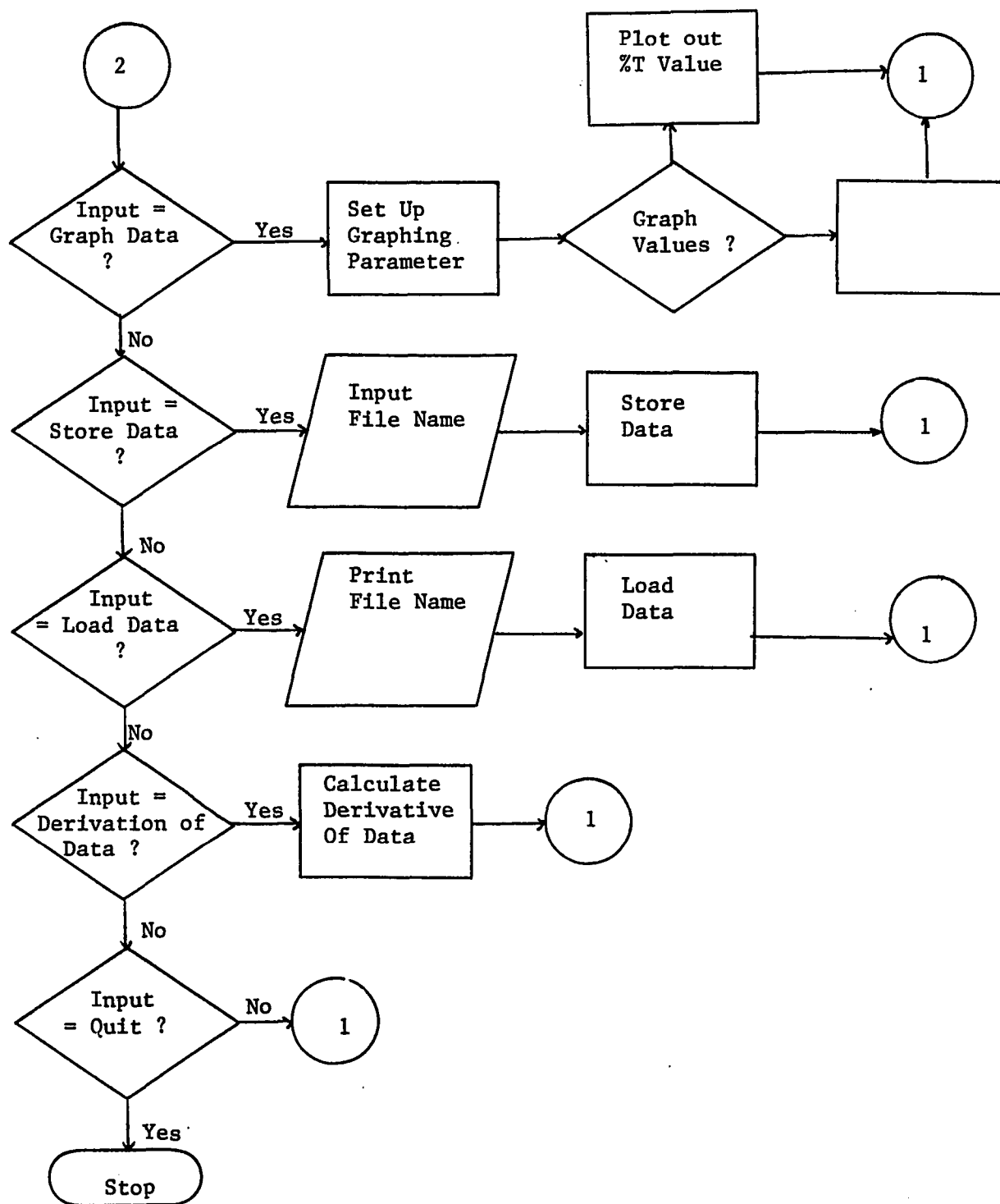


Figure 2D. Continued

REFERENCES

1. Szabadvary, T. History of analytical chemistry. New York: Pergamon Press, 1966, 318-344.
2. Mika, J. & Torok, T. Analytical emission spectroscopy, New York: Crane, Russak & Company, Inc., 1974, 401-509.
3. Skoog, D.A. & West D.M. Principles of instrumental analysis, Chicago: Holt, Rinehart and Winston, Inc., 1971, 27-66.
4. Rao, C.N.R. Ultra-violet and visible spectroscopy, 2nd ed., New York: Plenum Press, 1967.
5. Majer, J.R. & Azzouz, A.S.P. (1980) Talanta, 27, 549-556.
6. Olsen, E.D. Modern optical methods of analysis. New York: McGraw-Hill Book Company, 1975.
7. Hewlett Packard. "8450-A UV-VIS Spectrophotometer", Palo Alto, pp. 1-11.
8. Rofin Inc., (1981), Anal. Chem., 53, 1105A.
9. Gangwer, T., Schoener, G. & Smol, (1981), B. Amer. Lab, 13(9), 36-40.
10. Walling, P.L., Gentile, T.E. & Gudat, A.E. (1982), B. Amer. Lab, 14(2), 22-32.
11. Glenn, T., Brown, J., Kohler, V. & Brenner, N. Amer. Lab., 1982, 14(3), 48-54.
12. Wu, A.H.B., Rotunno, T. & Malmstadt, H.V. (1981) B. Amer. Lab., 13(9), 16-34.
13. Genshaw, M.A. & Rogers, R.W. (1981) B. Amer. Lab., 53, 1949-52.
14. Dolan Jenner Industries. Handbook of fiber optic applications.
15. Bendix Corp., Mosaic Fabrications Division. Fiber optic handbook, Sturbridge, MA: 1968.
16. Siegmund, W.P. Fiber optics: Principles, properties and design considerations, Southbridge, MA: American Optical Company, 1962.

17. Bensinger, M.G. The design, construction, and application of a multibeam fiber optics photometric titrator, M.S. Thesis, Western Michigan University, 1970.
18. Mellier-Smith, C.M. (1980) J. Chem. Ed., 57(8), 574-579.
19. Melles Griot. Optics guide 2, Irvine, CA: 1981.
20. Driscoll, W.G. & Vaughan, W. (Eds.). Handbook of optics, New York: McGraw-Hill Book Company, 1978.
21. Raychem Corporation of America, Maxlight Fiber Optic Division, Applications bulletin H-51160. Phoenix, AZ., 1982, 1-2.
22. American Optical Corporation. Applications bulletin S-969. Southbridge, MA., 1969, 1-2.
23. Hecht, J. (1982), Technology, 2(2), 40-51.
24. American Optical Corporation. Applications bulletin A11-73. 1973, 1-9.
25. Chabay, I. (1982), Anal. Chem., 54(9), 1071-1080A.
26. Crum, J.K. (196), Anal. Chem., 41, 26-32A.
27. Stock, J.T. (1970), J. Chem. Ed., 47(4), 311.
28. Munsinger, R.A. Fiber optic probe colorimeters eliminate manual color measurement. Westbury, NY: Brinkman Instruments Inc., 1981, 1-2.
29. Munsinger, R.A. Colorimetric/turbidimetric analyzers. Westbury, NY: Brinkman Instruments Inc., 1981, 1-6.
30. Munsinger, R.A. Fiber-optic colorimetry. Westbury, NY: Brinkman Instruments Inc., 1981, 1-6.
31. E.G. & G. Reticon, Applications Bulletin 97250. Sunnyvale, CA., 1978, 105.
32. Warren, M.W., Avery, J.P. & Malmstadt, H.V. (1982), Anal. Chem., 54, 1826-1828.
33. Analogic Corp. Applications bulletin BR-1021, Wakefield, MA: 1979, 1-2.
34. Malmstadt, H.V., Enke, C.G. & Crouch, S.R. Electronics and instrumentation for scientists. Reading, MA: Benjamin/Cummings Publishing Co., Inc., 1981, 383-385.

35. Hnatek, E. A user's handbook of D/A and A/D converters. New York: John Wiley & Sons, 1976, 4-19.
36. Rofin Inc. Series 6000 spectrolyzer fast spectral scanner, Marlboro, MA: 1983.
37. Hendrick, C.E. (1965), J. Chem. Ed., 42(9), 479-80.
38. Hamn, R.E. (1963), J. Am. Chem. Soc., 75, 5670-72.
39. Skoog, D.A. & West, D.M. Analytical chemistry: An introduction, 2nd ed. New York: Holt, Rinehart and Winston, Inc., 1965, 14-19.
40. Diehl, H. Calcein calmagite and O,O-dihydroxyazobenzene titrimetric colorimetric and fluorometric reagents for calcium and magnesium. Columbus, OH: G. Frederick Smith Chemical Company, 1964, 214-237.